

AD-A187 750

POA ENGINEERING SANTA ANA CA  
PATCHES-III. USER'S GUIDE FOR INVOLUTE COMPOSITES.(U)  
AUG 81 E L STANTON, T E KIPP  
POA-1437-00-02

F/8 21/8

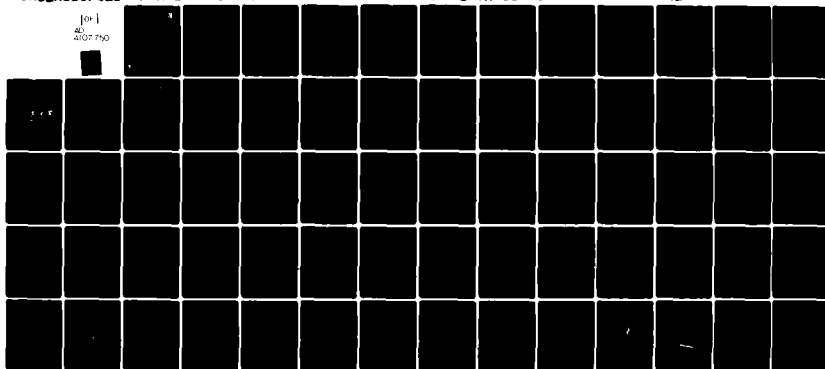
F04611-78-C-0082

UNCLASSIFIED

AFRPL-TR-81-43

NL

[OF]  
AL  
0107 750



END

DATE

FILED

02

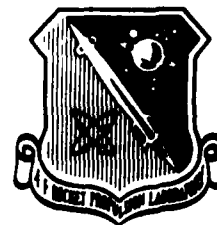
DTIC

**LEVEL II**

(2)

AFRPL-TR-81-43

PDA TR-1437-00-02



**PATCHES-III**

**USER'S GUIDE FOR INVOLUTE COMPOSITES**

Authors: E. L. Stanton  
T. E. Kipp

PDA Engineering  
1560 Brookhollow Drive  
Santa Ana, CA 92705

**DTIC**  
**ELECTE**  
NOV 27 1981

August 1981

APPROVED FOR PUBLIC RELEASE; DISTRIBUTION UNLIMITED

The AFRPL Technical Services Office has reviewed this report, and it is releasable to the National Technical Information Service, where it will be available to the general public, including foreign nationals.

Prepared for

AIR FORCE ROCKET PROPULSION LABORATORY  
DIRECTOR OF SCIENCE AND TECHNOLOGY  
AIR FORCE SYSTEMS COMMAND  
EDWARDS AFB, CALIFORNIA 93523

**8111 24 120**

AD A107700

ONE FILE COPY

## NOTICES

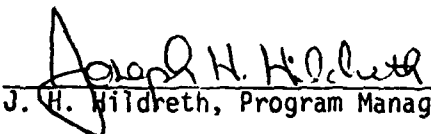
When U.S. Government drawings, specifications, or other data are used for any purpose other than a definitely related Government procurement operation, the Government thereby incurs no responsibility nor any obligation whatsoever, and the fact that the Government may have formulated, furnished, or in any way supplied the said drawings, specifications or other data, is not to be regarded by implication or otherwise, or in any manner licensing the holder or any other person or corporation, or conveying any rights or permission to manufacture, use, or sell any patented invention that may in any way be related thereto.

## FOREWORD

This report was prepared by PDA Engineering, Santa Ana, California under Contract F04711-78-C-0082, the Finite Element Spiral Ply Composites Program. The report was prepared for the Air Force Rocket Propulsion Laboratory, Edwards Air Force Base, CA 93523. Mr. Joseph Hildreth was the program manager.

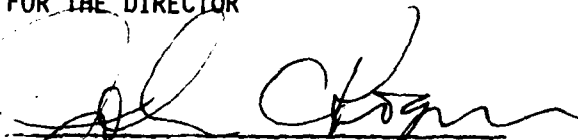
This is the final technical report covering work performed from October 1978 to January 1981 in accordance with CDRL Item No. 5.

This report is approved for release and distribution in accordance with the distribution statement on the cover and on the DD Form 1473.

  
J. H. Hildreth, Program Manager

  
Dr. C. W. Hawk, Chief  
Nozzle Technology Section

FOR THE DIRECTOR

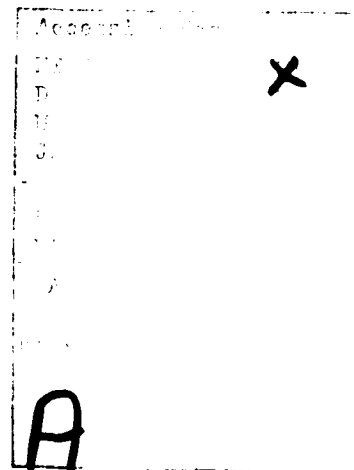
  
JOHN C. KOGER, Lt Colonel, USAF  
Deputy Director, Solid Rocket Division

REPORT DOCUMENTATION PAGE		READ INSTRUCTIONS BEFORE COMPLETING FORM
1. REPORT NUMBER AFRPL-TR-81-43	2. GOVT ACCESSION NO. AD-A107750	3. RECIPIENT'S CATALOG NUMBER
4. TITLE (and Subtitle) PATCHES-III User's Guide for Involute Composites		5. TYPE OF REPORT & PERIOD COVERED PROGRAM DOCUMENTATION OCTOBER 1978-APRIL 1981
		6. PERFORMING ORG. REPORT NUMBER PDA 1437-00-02
7. AUTHOR(s) E. L. Stanton and T. E. Kipp		8. CONTRACT OR GRANT NUMBER(s) F04611-78-C-0082
9. PERFORMING ORGANIZATION NAME AND ADDRESS PDA Engineering 1560 Brookhollow Drive Santa Ana, CA 92705		10. PROGRAM ELEMENT PROJECT, TASK AREA & WORK UNIT NUMBERS 305912 DH
11. CONTROLLING OFFICE NAME AND ADDRESS Air Force Rocket Propulsion Laboratory Edwards Air Force Base, CA 93523		12. REPORT DATE August 1981
		13. NUMBER OF PAGES 61
14. MONITORING AGENCY NAME & ADDRESS (if different from Controlling Office)		15. SECURITY CLASS (of this report) Unclassified
		15a. DECLASSIFICATION/DOWNGRADING SCHEDULE
16. DISTRIBUTION STATEMENT (of this Report)  Approved for public release; distribution unlimited.		
17. DISTRIBUTION STATEMENT (of the abstract entered in Block 20, if different from Report)		
18. SUPPLEMENTARY NOTES		
19. KEY WORDS (Continue on reverse side if necessary and identify by block number) Exit Cone Involute Composite Involute Billet Carbon-Carbon Finite Element		
20. ABSTRACT (Continue on reverse side if necessary and identify by block number) A user's guide is provided for the nozzle analyst who needs to use the computer program PATCHES-III to model an involute component, but who does not want to become expert in all the modeling capabilities of the program. The analyst is expected to have a finite element background and should be familiar with how an involute is constructed. Models of test cylinders, involute billets and beam specimens excised from involute rings are described in detail. The bulk data input for these models are annotated and the output is illustrated with computer plots.		

411772

## TABLE OF CONTENTS

<u>Section</u>	<u>Page</u>
1.0 INTRODUCTION	1
1.1 Spiral Ply Composite Analysis	1
1.2 Exit Cone Ply Pattern Analysis	4
2.0 HOW TO MODEL AN INVOLUTE	7
2.1 Modeling the Geometry	7
2.2 Modeling the Properties	13
3.0 HOW TO ANALYZE YOUR INVOLUTE MODEL	27
3.1 Modeling the Boundary Conditions	27
3.2 Modeling the Loads	31
3.3 Case Control Input	32
4.0 APPLICATIONS AND ILLUSTRATIONS	37
4.1 Involute Test Cylinder	37
4.2 Involute Billet Analysis	46
4.3 Involute Beam Specimen	50
5.0 UNDERSTANDING THE RESULTS	55
5.1 Printed Output	55
5.2 Plotted Output	57
6.0 REFERENCES	61



## LIST OF ILLUSTRATIONS

<u>Figure</u>	<u>Page</u>
1. Involute Cone Construction	2
2. Material Coordinate Rotated to Structural Coordinates	3
3. Warp/Fill Autopsy Fingerprints	6
4. Pagano Exact Involute Paper Cone	8
5. Model Cone Grid Points	9
6. Model Cone Patches	10
7. Model Cone Hyperpatches	11
8. Contoured Cone Hyperpatches	14
9. Pagano Exact Cone Ply Pattern	18
10. Arc Angle Variation Axially	19
11. Helix Angle Variation Axially	20
12. Tilt Angle Variation Axially	21
13. Model Cone with Cylindrical Insert	29
14. Involute Test Cylinder Gage Section Model	39
15. Involute Test Cylinder Deformations in Torsion	40
16. Involute Test Cylinder Shear Stress Contours	41
17. Exact Involute Billet Ply Pattern	44
18. Exact Involute Billet Model	45
19. Involute Billet Shear Stress Contours	48
20. Involute Billet Normal Stress Contours	49
21. Involute Beam Specimen Model	51
22. Involute Beam Fill Stress Contours	53
23. Involute Beam Shear Stress Contours	54
24. ENEC Joint Finite Element Model Deformations	58
25. Contour Stress Results for a Single CCX Element	59
26. Involute Cylinder Shrinkage Study	60

# LIST OF TABLES

<u>Table</u>		<u>Page</u>
1.	Geometry Directives for Pagano Cone	12
2.	Graphite Phenolic Nominal Post Cure Properties	16
3.	Temperature Dependent Material Input	17
4.	Material Geometry DATAG Direct Input	23
5.	Material Geometry Data Hyperpatch Construction	24
6.	Finite Element Property and Connectivity Definition	25
7.	Sliding Interface Constraint Modeling	30
8.	Element Temperature Modeling	30
9.	Element Pressure Load Modeling	33
10.	Case Control Input for a Dry Run	33
11.	Case Control Input for Multiple Subcases	35
12.	Involute Cylinder Bulk Data Model	38
13.	Involute Test Cylinder Case Control	43
14.	Involute Billet Geometry Model	46
15.	Involute Billet Temperature Dependent Properties Input	47
16.	Billet Finite Element Data	47
17.	Involute Beam Modeling Directives	52
18.	PATCHES-III Output Format for CCX Elements	56

## DEFINITION OF SYMBOLS

$C$	Involute Constant; $r \sin \alpha = C$
$E_{ii}$	Extensional Elastic Constants
$e_i$	Cartesian Coordinates Unit Vectors
$\underline{f}$	Fill Fiber Direction
$G_{ij}$	Shear Moduli
$\underline{i}, \underline{j}, \underline{k}$	Cylindrical Coordinate Unit Vectors
$\underline{n}$	Ply Surface Normal Direction
$N$	Number of Plies in Billet
$\underline{s}$	Ply Surface Tangent Vector in $\underline{i}, \underline{j}$ Plane (Hoop)
$\underline{t}$	Ply Surface Tangent Vector in $\underline{j}, \underline{k}$ Plane (Axial)
$T$	Ply Thickness
$U_i$	Displacement Vector Components
$\underline{w}$	Warp Fiber Direction
$Z_i$	Cartesian Position Vector Components
$\alpha$	Involute Arc Angle; $\alpha = \text{ACOS}(\underline{i} \cdot \underline{t})$
$\alpha_{ij}$	Coefficients of Thermal Expansion
$\gamma$	Tilt Angle; $\gamma = \text{ACOS}(\underline{t} \cdot \underline{k})$
$\theta$	Second Euler Angle in the PATCHES-III Material Geometry Definition. (Also used for circumferential cylindrical coordinate.)
$\nu_{ij}$	Poisson Ratios
$\xi_i$	Parametric Coordinates in PATCHES-III
$\phi$	Helix Angle; $\text{ACOS}(\underline{t} \cdot \underline{w})$ (Also used for third Euler angle in PATCHES-III.)
$\psi$	First Euler Angle in PATCHES-III Material Geometry Definition.

## 1.0 INTRODUCTION

This user's guide is intended for the nozzle analyst who wants to use PATCHES-III to model an involute component, but who does not want to become expert in all the modeling capabilities of the program. Those interested in a complete description of all available options in this general 3D code should consult the User's Manual. The analyst should have a general understanding of finite element methods, experience with another finite element program would be helpful, and the analyst should be familiar with how an involute is constructed. The user's guide, together with this general background, should allow a nozzle analyst to model an involute component and compute its stress-strain response in the linear elastic range.

### 1.1 Spiral Ply Composite Analysis

A laminated composite with curvature and finite thickness has continuously varying fiber directions. Only in very special cases, such as a polar weave, do these directions align with structural coordinate directions. It is this variation in fiber direction or alignment that causes the unusual response modes and analysis difficulties in spiral ply composites. When the composite is laminated from identical plies, it is only necessary to know the orientation of the material axes at every material point in order to analyze its elastic response. This situation is typical of involute construction, Figure 1, and the matrix transformations necessary to compute material properties in structural coordinates are described in Reference 1. When different ply materials are laminated in a repeating arrangement to form the composite, a preprocessor like PATRAN, can be used to compute effective ply properties for the analysis. In both instances the local material axes are defined by three rotations (Euler angles) that take material coordinates (w,f,n) into structural coordinates ( $\theta, r, z$ ) as illustrated in Figure 2. These rotation angles change continuously with position which led to the development of a finite element with material orientation defined by Euler angle distribution functions. This is the key step in modeling spiral ply composites with minimum data input. It allows the finite element mesh to be determined on the basis of the material response as opposed to the material distribution.

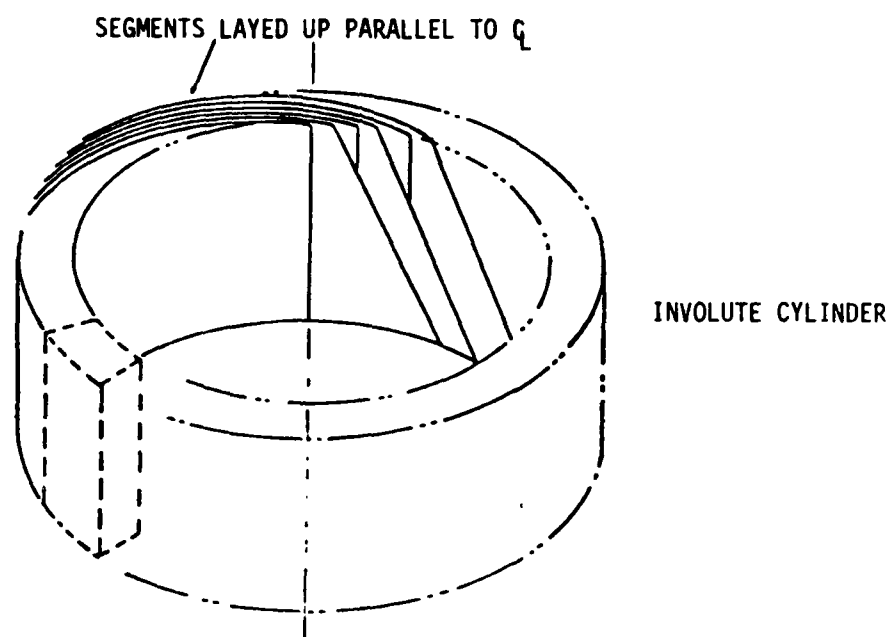
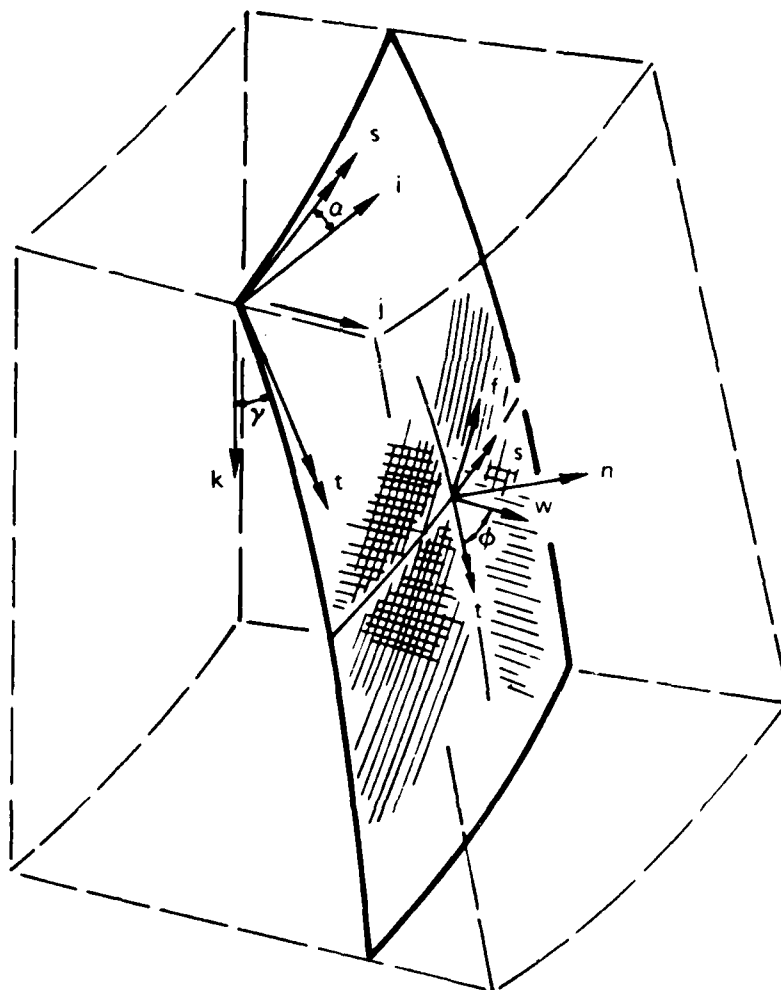


Figure 1. Involute Cone Construction



8000836

Figure 2. Material Coordinate Rotated to Structural Coordinates

## 1.2 Exit Cone Ply Pattern Analysis

Given a finite element capable of modeling spiral ply composites, next we must determine specific Euler angle distribution functions. In the case of involute construction these functions can be determined "exactly" for a convolute ply pattern, Reference 2. When piecewise convolute construction, Reference 3, is used the same formulas apply but with the involute constant changed by the local tilt angle  $\gamma(Z)$ . Only the fixed convolute construction produces an involute surface of single curvature that can be formed without ply distortion. However, this distortion is small in a well designed part and the ideal material analysis described here accounts only for the local tilt angle changes.

The ply pattern design parameters that determine its developed shape, as well as fiber directions in the part, can be shown to be,

$$\begin{array}{lcl}
 \begin{array}{l}
 C - \text{Involute Constant} \\
 N - \text{Number of Plies} \\
 T - \text{Ply Thickness} \\
 R_1(Z), R_2(Z) - \text{Billet or Cone Profile} \\
 C(Z) - \text{Variable Involute Constant}
 \end{array}
 & \left. \begin{array}{l} \\ \\ \\ \\ \end{array} \right\} \begin{array}{l} \text{Exact} \\ \text{Convolute} \\ \\ \\ \text{Piecewise} \\ \text{Convolute} \end{array} & \left. \begin{array}{l} \\ \\ \\ \\ \end{array} \right\} \begin{array}{l} \text{Ply Pattern} \\ X(r,z) \\ Y(r,z) \end{array}
 \end{array}$$

where the Euler angles at any axial station  $Z$  have a radial distribution that is very nearly linear in  $r$

$$\begin{aligned}
 \alpha(r) &= \text{ARCSIN } (c/r) \\
 \gamma(r) &= \text{ARCTAN } (A/\cos \alpha)
 \end{aligned}$$

$$\phi(r) = \phi_0 + \int_{\alpha(r_0)}^{\alpha(r)} \frac{A[(3+A^2) \cos^4 \alpha - 3 \cos^2 \alpha + 1]^{1/2}}{(A^2 + \cos^2 \alpha) \sin^2 \alpha} d\alpha$$

with

$$A = (4\pi^2 C^2 - N^2 T^2)^{1/2} / NT$$

When  $\alpha$  is small, which is true of virtually all exit cones,

$$\phi(r) \cong \phi_0 + \left( \frac{180}{\pi} \right) (A(r-r_0)/c) \sqrt{1+A^2}$$

These are the basic input data for a PATCHES-III finite element model of an

ideal involute composite formed using a single base ply pattern. The as-built fiber directions can deviate significantly from these values in cone-cylinder transition regions if, for example, rapid changes in  $C(Z)$  occur, Reference 1, or when other material distortions are present. At present these effects must be determined from autopsy specimens as in the work of Buch and Pfeifer, Reference 4, which maps the as-built material distortions, Figure 3. When these data are available, PATCHES-III can model these effects.

The Euler angle distribution within an individual element in PATCHES-III can be constant, linear, quadratic or cubic. This allows many involute components to be modeled with a single finite element through the thickness. Modeling information on how to input Euler angle data from a ply pattern analysis to the program is described in the sections that follow. The source of the data, measured or computed, does not change the way in which it is input to the program.

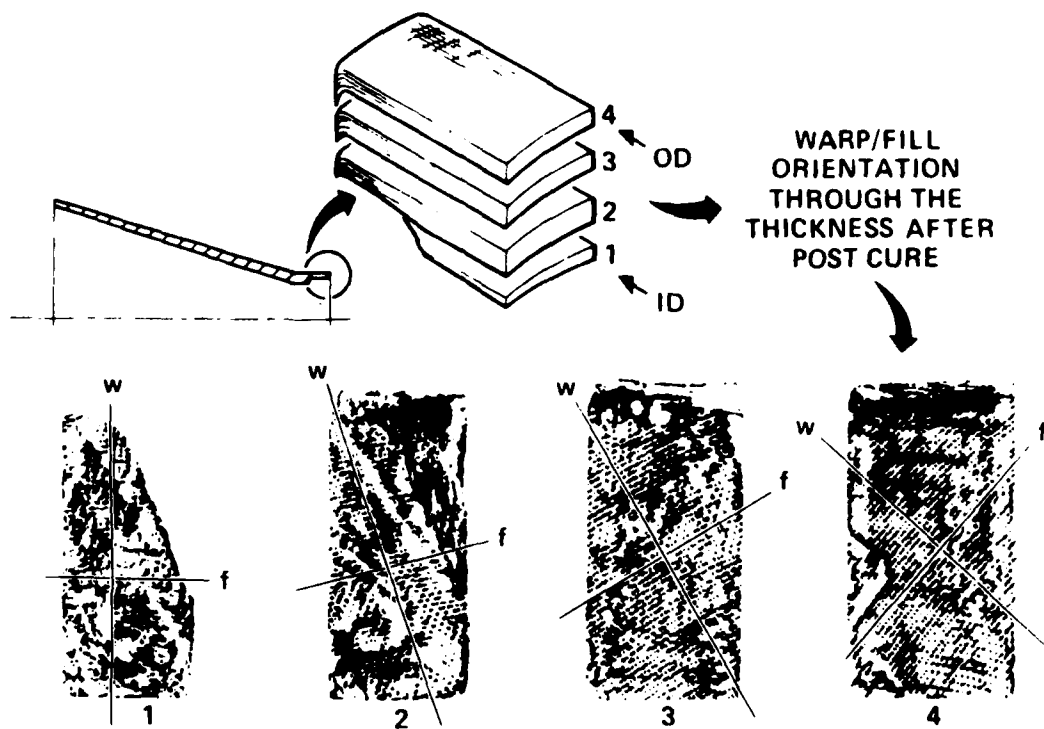


Figure 3. Warp/Fill Autopsy Fingerprints

## 2.0 HOW TO MODEL AN INVOLUTE

The finite elements in PATCHES-III are truly three-dimensional solid elements, which tends to increase the input data requirements per individual finite element in comparison to a two-dimensional SAAS-III finite element. However, most of the additional data are generated by the program from benchmark data using precoded construction operations, References 5 and 6. The use of these operations to construct an involute body of revolution is especially simple as we now describe.

### 2.1 Modeling the Geometry

To create a simple geometric shape representing a section of an involute billet, we first create a model of its cross-section (called a patch) and direct the program to rotate that two-dimensional shape to create a segment of a solid of revolution. The benchmark data in this case are the coordinates of the four corner nodes. To illustrate the procedure, let us model the Pagano exact involute cone shown in Figure 4. In this case, the billet and net part are the same dimension because of the incompressible material used in its construction.

Seven grid points are input as benchmark coordinate data for the entire model, Figure 5. These have the grid identification numbers (GID's) 1, 3, 13, 21, 23, 28, 33 where any convenient numbering system could have been used. The patches that model a meridional cross-section of this billet are all straight sided quadrilaterals drawn between the grid points. Coordinates for the 26 grid points not directly input are generated using five line directives that uniformly subdivide the distance between benchmark points. The LINEPC directive performs this operation. Next, twelve (12) patch directives are used to create a continuous two-dimensional model of the cross-section. For this shape, the PATCHQ directive is used to generate straight sided quadrilaterals, Figure 6. Now all that remains is to create 12 three-dimensional solid elements by rotating the 12 patches. The HPR directive performs this operation for rotation about a coordinate axis. Note the resulting model, Figure 7, is a continuous representation of the geometry with 12 curvilinear hexahedra (hyper-patches) constructed without recourse to the mathematics used by the program. The entire set of input used to create the solid geometry model is listed in Table 1.

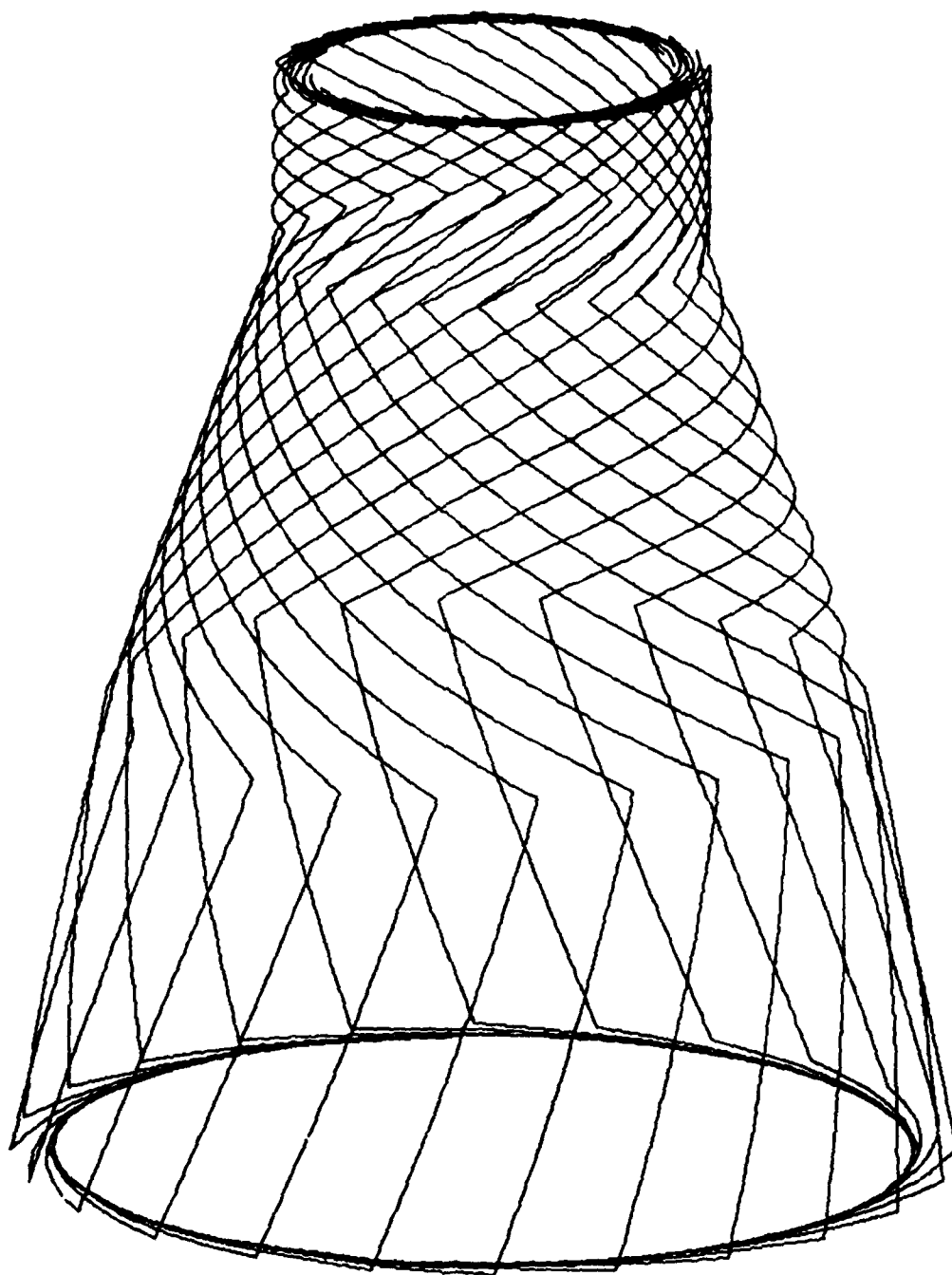


Figure 4. Pagano Exact Involute Paper Cone

8100247

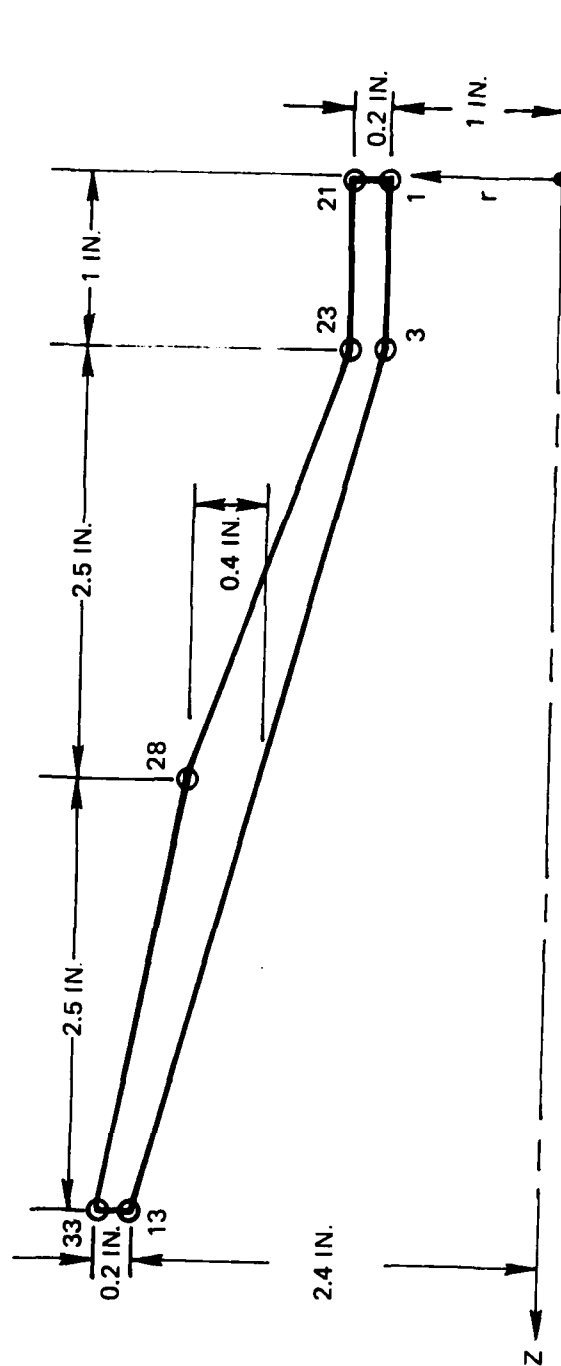
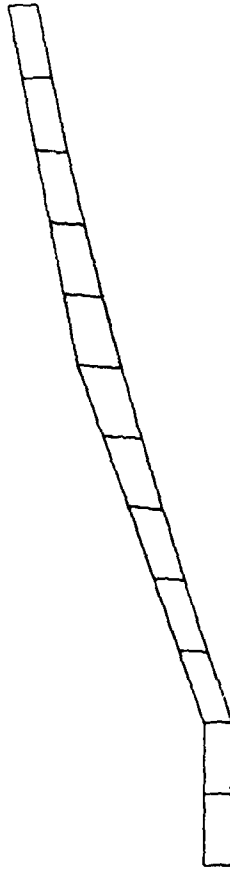


Figure 5. Model Cone Grid Points

8100240

PROGRAM EXACT INVOLUTE CONE  
 CONTOURED CONE PROFILE



VIEW ANGLES	0.00	90.00	0.00
ELEMENT	FACE		
1	S		
2	S		
3	S		
4	S		
5	S		
6	S		
7	S		
8	S		
9	S		
10	S		
11	S		
12	S		

8100248

Figure 6. Model Cone Patches



---

TABLE 1. GEOMETRY DIRECTIVES FOR PAGANO CONE

---

GRID, 1, , ,1.0,0.0  
 GRID, 3, , ,1.0,1.0  
 GRID, 13, , ,2.4,6.0  
 GRID, 21, , ,1.2,0.0  
 GRID, 23, , ,1.2,1.0  
 GRID, 28, , ,2.1,3.5  
 GRID, 33, , ,2.6,6.0

LINEPC, 1, 1, 2, 3  
 \*LINEPC, 2, 3 THRU 13  
 LINEPC, 3,21,22,23  
 LINEPC, 4,23 THRU 28  
 LINEPC, 5,28 THRU 33

PATCHQ, 1, 1, 2,22,21  
 PATCHQ, 2, 2, 3,23,22  
 PATCHQ, 3, 3, 4,24,23  
 PATCHQ, 4, 4, 5,25,24  
 PATCHQ, 5, 5, 6,26,25  
 PATCHQ, 6, 6, 7,27,26  
 PATCHQ, 7, 7, 8,28,27  
 PATCHQ, 8, 8, 9,29,28  
 PATCHQ, 9, 9,10,30,29  
 PATCHQ, 10,10,11,31,30  
 PATCHQ, 11,11,12,32,31  
 PATCHQ, 12,12,13,33,32

HPR, 1, 1, , , ,0.0,15.0,-3  
 HPR, 2, 2, , , ,0.0,15.0,-3

↓

---

HPR, 12,12, , , ,0.0,15.0,-3

---

\*Alternate Construction for Contoured Cone

LINEGR, 2,3,0,-32.0038,12.8814,  
 1,-32.0038,12.8814, ,  
 8.4889,0.0,3 THRU 13

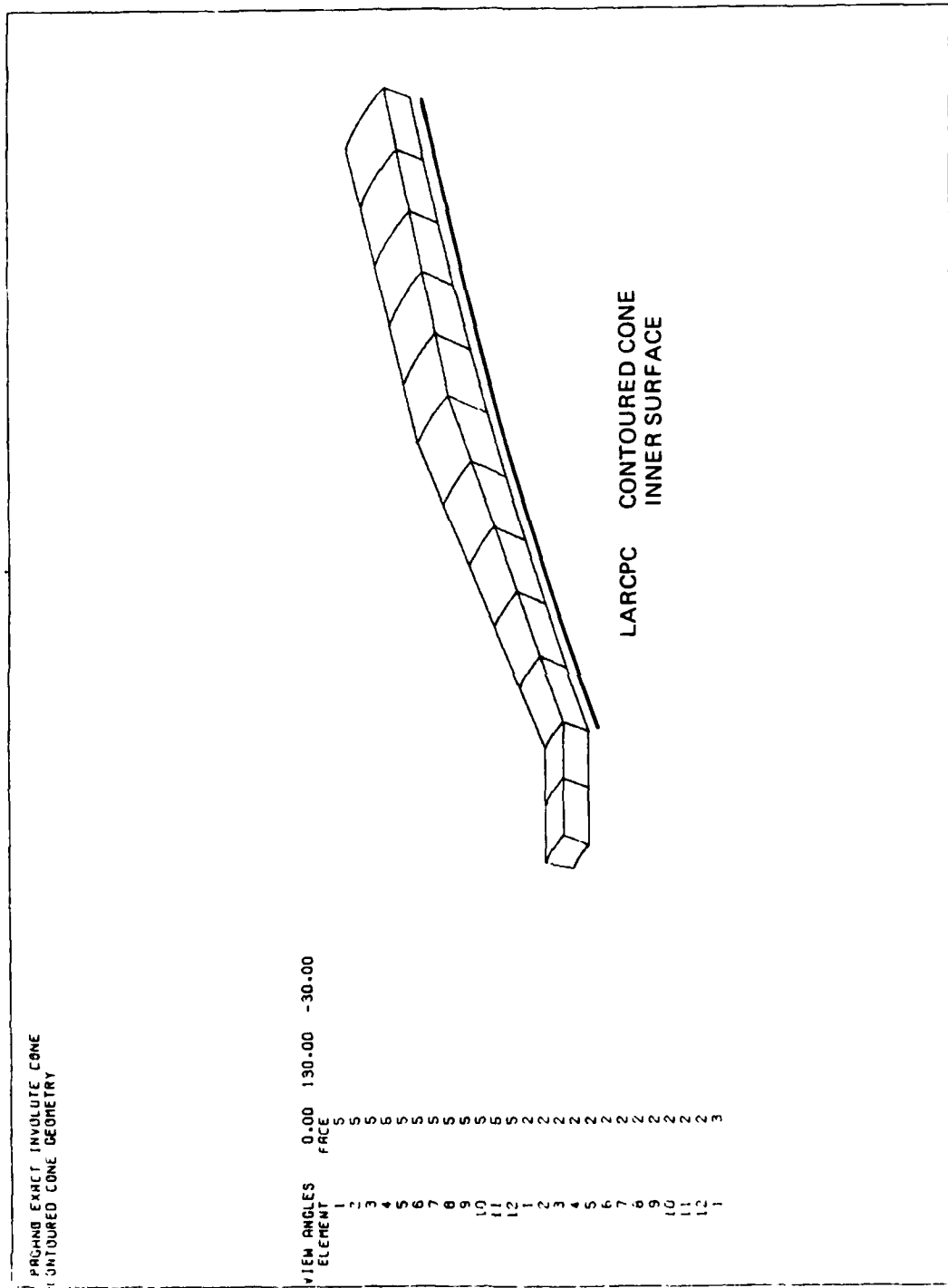
---

The geometry model just created has no implied conventions if the 64 node tricubic (CCC) finite element is used. However, when the 16 node axisymmetric finite element option (CCX) is used, the circumferential coordinate direction must be defined by the third parametric coordinate. This convention must be observed in defining finite element connectivity, but that is the subject of another chapter. Our purpose here is to introduce construction concepts and procedures that can be used to create axisymmetric geometries with PATCHES-III directives. After the basic modeling concepts have been illustrated, we will come back to the finite element issues.

Suppose that the inner surface of our model exit cone had a contoured shape defined by the arc of a great circle instead of the straight cone design. We need only change one line directive and delete one grid directive to create the geometry for this exit cone billet, Figure 8. The line defining the inner shape of the cone is created by rotating grid point 3 using the LINEGR directive. The rotation axis is defined by the chord length between grid points 3 and 13 and by the condition that the arc be parallel to the external surface at the axial stations associated with these two grid points. In this construction grid point, 13 is computed by the LINEGR directive rather than input on a GRID directive. We could input both directives, but the two sets of coordinates for 13 would have to agree to five places to avoid a fatal error message. (Redundant input is allowed in most cases but not recommended.) This billet illustrates how PATCHES-III constructs solid geometry for axisymmetric shapes from benchmark data. It is possible to examine the geometry using the DRY option before completing the model. When a graphics work station is available, a PATCHES-III plot code postprocessor can be used to view the model or any portion of the model and hardcopy plots can be made using the same input with another postprocessor. Previewing the model in either case is good practice, especially for complicated shapes.

## 2.2 Modeling the Properties

The involute construction process described earlier requires only one ply material and that is usually a prepreg made from a graphite fabric such as square weave WCA. A very readable description of carbon fabric composites that graphically illustrates the semantics of fiber technology may be found in Reference 7. The properties of an orthotropic ply material are input using a MATOR directive for engineering elastic constants and a MATAL directive for



5000250

Figure 8. Contoured Cone Hyperpatches

coefficients of thermal expansion. Typical values for a laminated WCA carbon phenolic material in the post-cured condition are given in Table 2 for temperatures up to 500°F. To model a temperature dependent property of any type, a data table function is used in PATCHES-III. The DTCS and DTPC directives that create these functions use spline interpolation and piecewise linear interpolation, respectively, between tabular input data versus temperature in this case. The material directives corresponding to MATOR and MATAI that use these data table functions are MATTO and MATTA. Input directives that represent the material data in Table 2 are shown in Table 3. Note that these properties are triaxial properties and not plane strain or plane stress properties. A number of other material directives for fully anisotropic and for isotropic materials are also available.

Next we must model the Euler angle data that define the unusual warp and fill fiber orientation produced by the involute construction process. These angles are computed normally by a preprocessor program using the equations described earlier for a convolute surface. On occasion the as-built orientations are available from an autopsy. In either case, parametric cubic models are used to represent the Euler angles over the volume of each finite element. These models are called data hyperpatches, and they are constructed from benchmark data using "data directives" equivalent to the geometric directives described in the last section. To illustrate the procedure, consider the Pagano cone again, but assume it had been made from a woven prepreg with a cured thickness of 0.01 inches. The exact ply pattern for a ninety-two (92) ply billet is shown in Figure 9, and the Euler angles as a function of axial station are shown in Figures 10, 11, and 12 for the inside surface and the outside surface, respectively. The radial distribution is linear for small arc angles to the same approximation that  $\alpha \cong \sin \alpha$ . Note also that the pattern is oriented on broadgoods such that  $\phi = 0$  at the inside of the billet at the aft end.

The data hyperpatches that define the hoop, radial and axial variations for each Euler angle normally can be created from grid point data similar to the geometry. The DATAG directive is used to input scalar data at individual grid points that the program stores by data set identification number. These data can then be referenced by DHPHEX directives to create trilinear models for each variable Euler angle for each finite element. The DATAG direct input directives for modeling the example cone's arc angle and helix angle data are shown

TABLE 2. GRAPHITE PNEOLIC NOMINAL POST CURE PROPERTIES\*

T	E11	E22	E33
70°	13.1 GP (1.90 msi)	8.8 GPa (1.27 msi)	3.1 GPa (0.45 msi)
200°	11.0 GP (1.60 msi)	7.4 GPa (1.07 msi)	2.6 GPa (0.38 msi)
300°	9.2 GP (1.33 msi)	6.1 GPa (0.89 msi)	2.2 GPa (0.32 msi)
400°	7.6 GP (1.10 msi)	5.1 GPa (0.74 msi)	1.8 GPa (0.26 msi)
500°	6.0 GP (0.87 msi)	4.0 GPa (0.58 msi)	1.4 GPa (0.21 msi)
	NU12	NU13	NU23
70°	0.19	0.12	0.09
500°	0.19	0.12	0.09
	G12	G13	G23
70°	5.5 GP (0.80 msi)	2.1 GPa (0.30 msi)	3.1 GPa (0.45 msi)
200°	4.6 GP (0.67 msi)	1.7 GPa (0.25 msi)	2.6 GPa (0.38 msi)
300°	3.9 GP (0.56 msi)	1.4 GPa (0.21 msi)	2.2 GPa (0.32 msi)
400°	3.2 GP (0.46 msi)	1.2 GPa (0.17 msi)	1.8 GPa (0.26 msi)
500°	2.6 GP (0.37 msi)	1.0 GPa (0.14 msi)	1.4 GPa (0.21 msi)
	$\alpha_{11} \times 10^6$	$\alpha_{22} \times 10^6$	$\alpha_{33} \times 10^6$
70°	2.7/°K (5.0/°F)	3.9/°K (7.0/°F)	8.3/°K (15.0/°F)
200°	2.4/°K (4.4/°F)	4.5/°K (8.1/°F)	7.9/°K (14.2/°F)
300°	1.8/°K (3.2/°F)	3.8/°K (6.9/°F)	6.2/°K (11.2/°F)
400°	1.2/°K (2.2/°F)	2.6/°K (4.6/°F)	2.7/°K (4.9/°F)
500°	.83/°K (1.5/°F)	1.6/°K (2.8/°F)	-.22/°K (-0.4/°F)

\*The Poisson ratios are assumed constant to 500°.

---

TABLE 3. TEMPERATURE DEPENDENT MATERIAL INPUT

---

DTPC, 1,70, 70,1.90+6,200,1.60+6,300,1.33+6, 400,1.10+6,500,0.87+6	}	EII
DTPC, 2,70, 70,1.27+6,200,1.07+6,300,0.89+6, 400,0.74+6,500,0.58+6		
DTPC, 3,70, 70,0.45+6,200,0.38+6,300,0.32+6, 400,0.26+6,500,0.21+6		
DTPC, 4,70, 70, 0.19,500, 0.19	}	NUIJ
DTPC, 5,70, 70, 0.12,500, 0.12		
DTPC, 6,70, 70, 0.09,500, 0.09		
DTPC, 7,70, 70,0.80+6,200,0.67+6,300,0.56+6, 400,0.46+6,500,0.37+6	}	GIJ
DTPC, 8,70, 70,0.30+6,200,0.25+6,300,0.21+6, 400,0.17+6,500,0.14+6		
DTPC, 9,70, 70, 5.0-6,200, 4.4-6,300, 3.2-6, 400, 2.2-6,500, 1.5-6	}	$\alpha$ IJ
DTPC,10,70, 70, 7.0-6,200, 8.1-6,300, 6.9-6, 400, 4.6-6,500, 2.8-6		
DTPC,11,70, 70,15.0-6,200,14.2-6,300,11.2-6, 400, 4.9-6,500,-0.4-6		

\*MATTO, 1, ,1,2,3,4,5,6,7,8,3

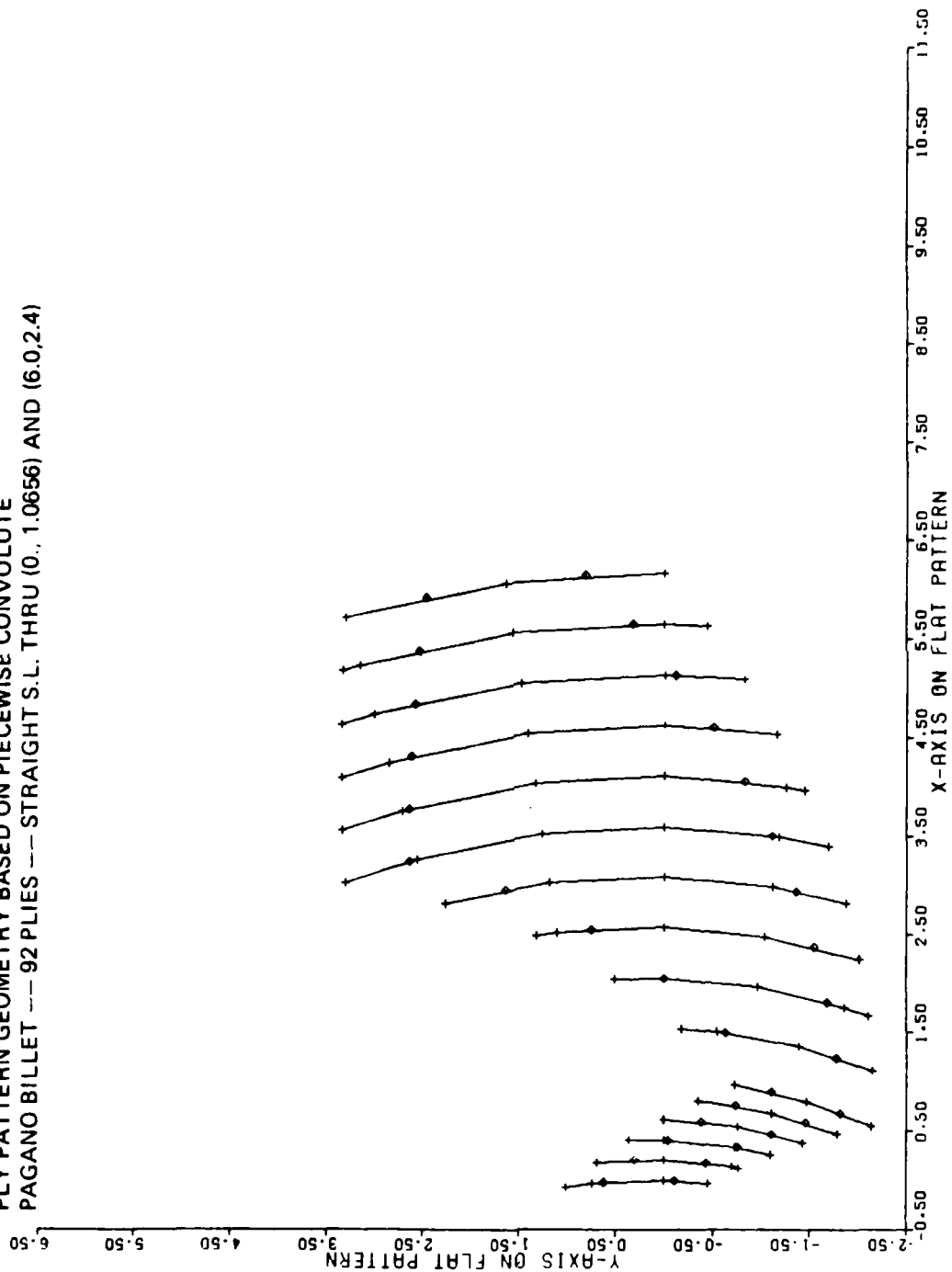
MATTA, 1, ,9,10,11

---

\*Note the same function is used for E33 and G23.

---

PLY PATTERN GEOMETRY BASED ON PIECEWISE CONVOLUTE  
 PAGANO BILLET --- 92 PLIES --- STRAIGHT S.L. THRU (0., 1.0656) AND (6.0,2.4)



8100251

Figure 9. Pagano Exact Cone Ply Pattern

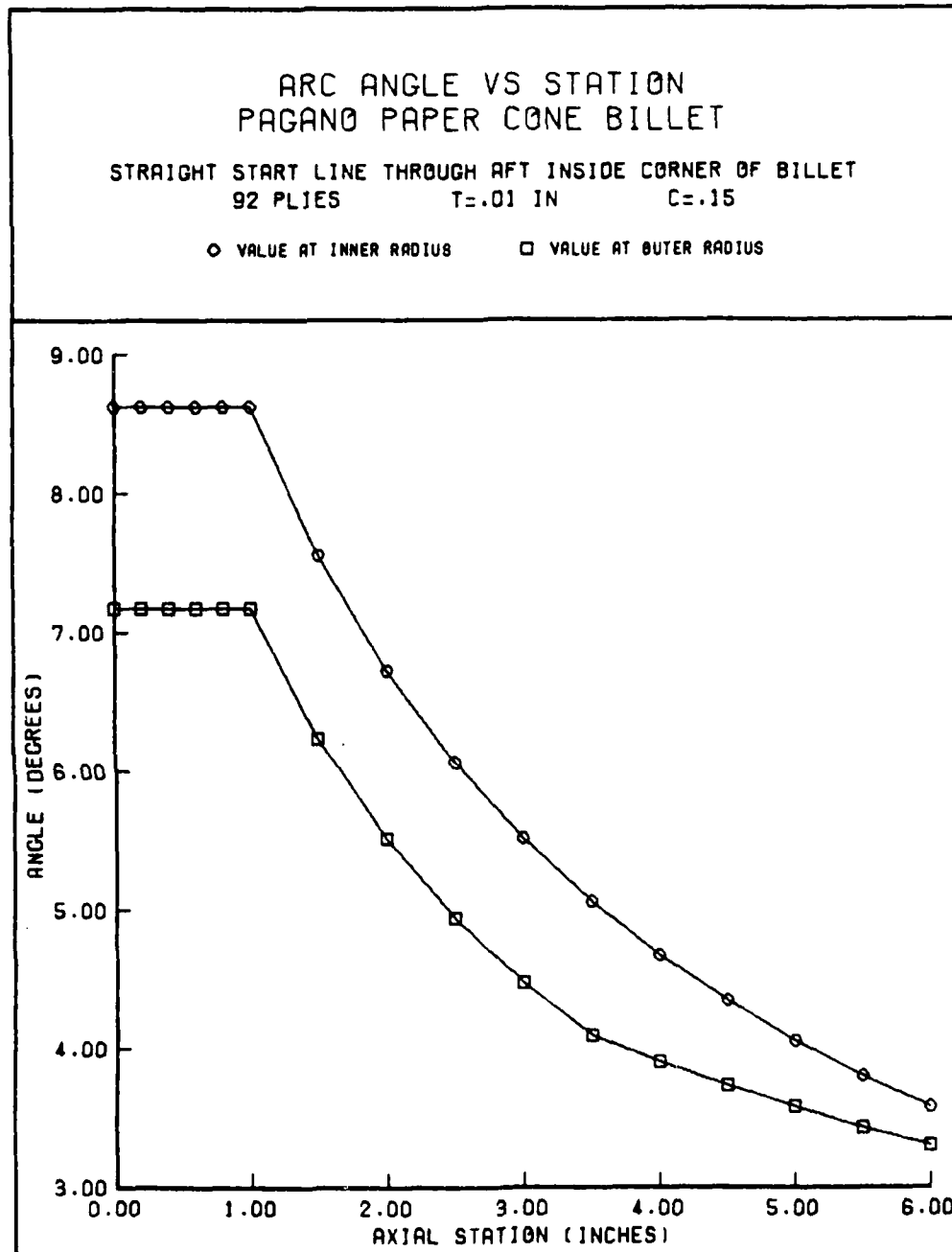
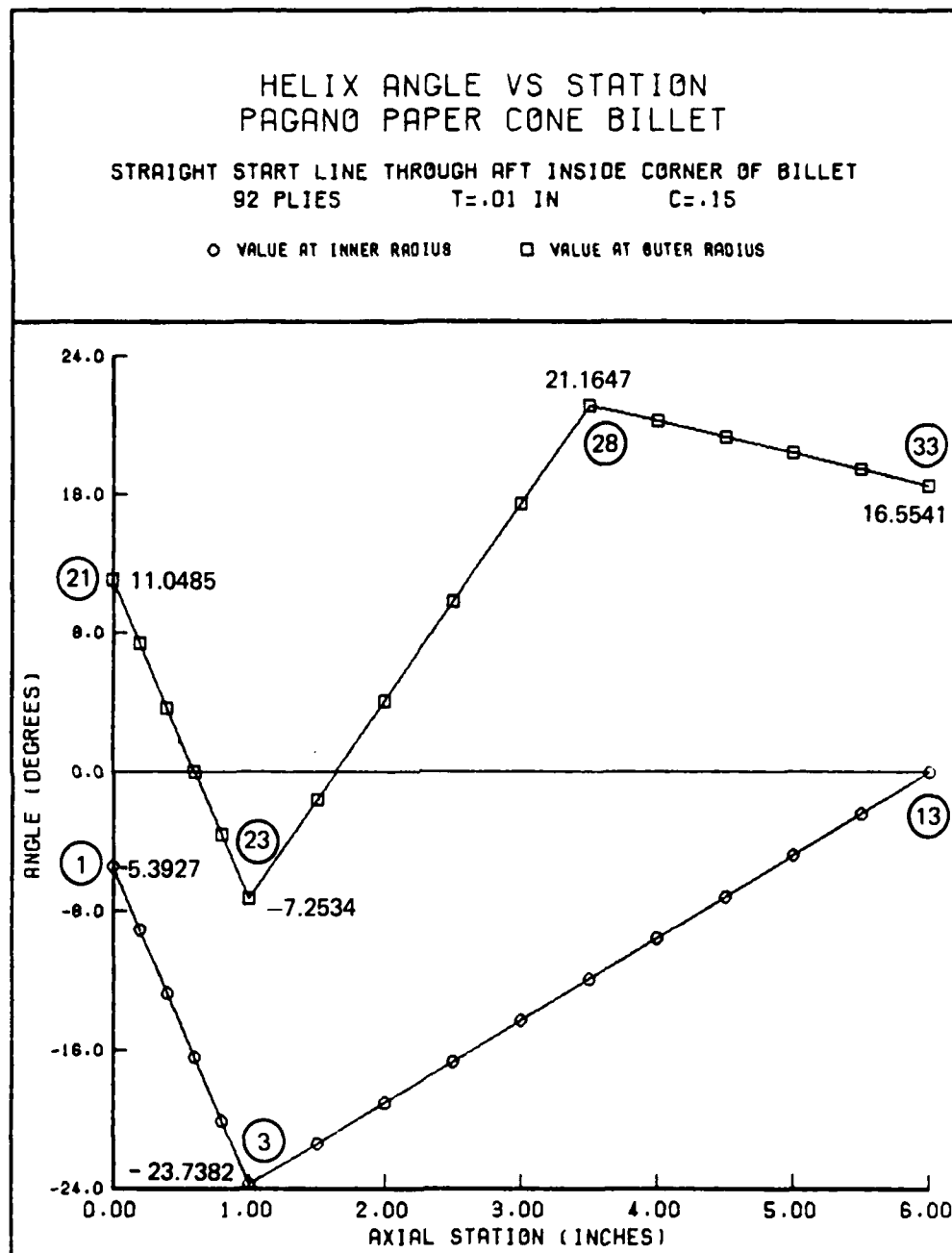


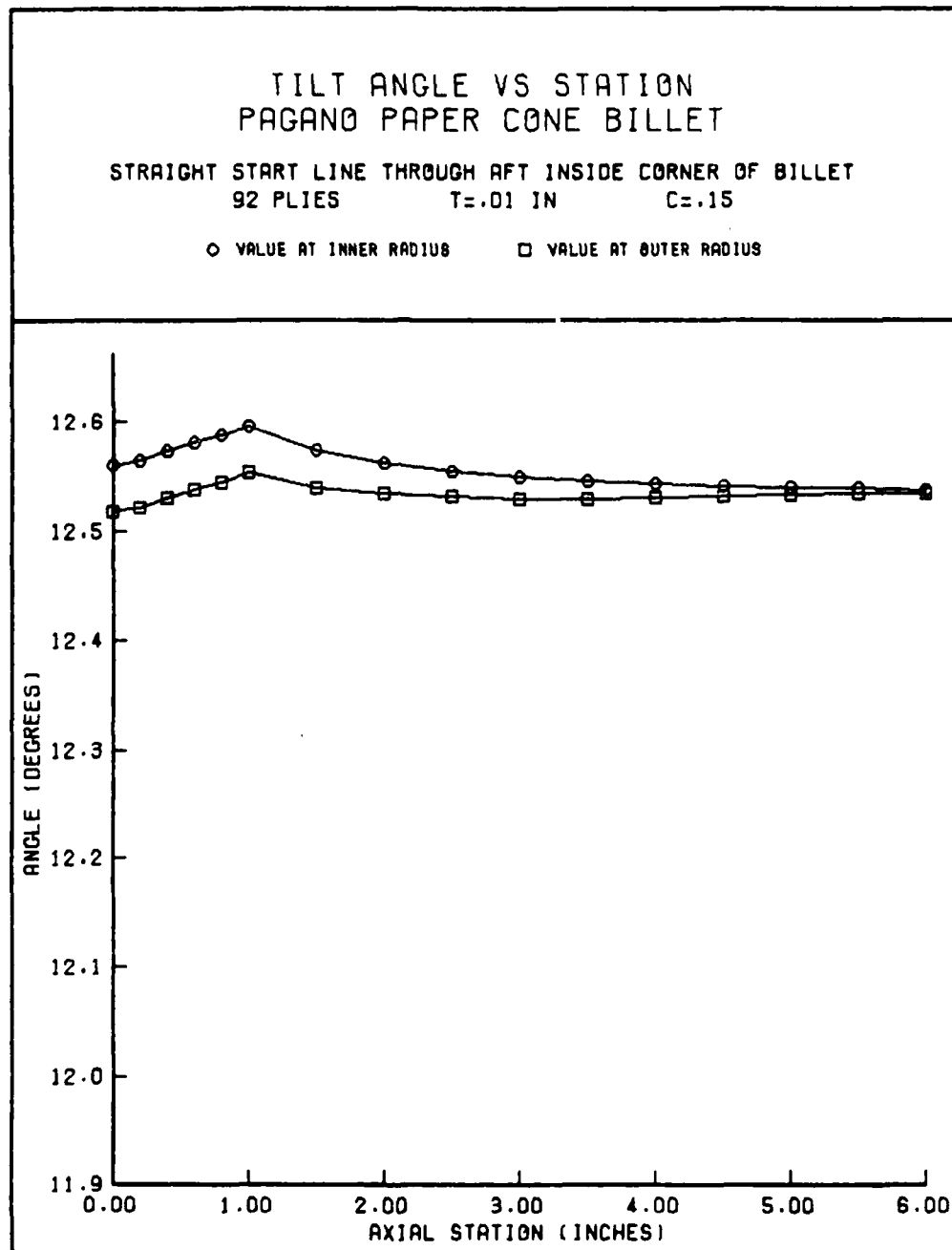
Figure 10. Arc Angle Variation Axially

8100252



8100254

Figure 11. Helix Angle Variation Axially



8100253

Figure 12. Tilt Angle Variation Axially

in Table 4. Note that the Euler angles used by PATCHES-III are related to  $\alpha$ ,  $\gamma$ , and  $\phi$  by

$$\psi = -(\alpha + \theta)$$

$$\theta = 90 - \gamma$$

$$\phi = 90 - \phi$$

where the arc angle,  $\alpha$ , is increased by the local circumferential coordinate,  $\theta$ , for grid points off the  $\theta = 0$  face. In the example problem grid points 101 through 133 all lie on the  $\theta = 15^\circ$  face of the model and have the same  $r, z$  coordinates as grid point 1 through 33. The DATAG input directives for data set one (the arc angle data) reflect this  $15^\circ$  difference between the entries for grid points 1 through 33 and grid points 101 through 133. Data at a few grid points were computed using the data line directive DLINPC for interpolation and more could have been, using PC data lines for  $\alpha(r)$ . The data line and data hyperpatches directives shown in Table 5 were kept elementary to focus attention on the concept of material geometry modeling. A data hyperpatch created from scalar data sets or any other source is not used until referenced by another directive in PATCHES-III. This allows the same data modeling system to service all properties that vary spatially over the structure.

The involute material construction is defined by the PPDE3 property directive for each element which specifies the material identification number and the Euler angles that relate the material axes to the reference axes. When the same material fills the element volume, which is true of most involutes, the material identification number references a single set of ply material properties. However, up to 64 different sets of elastic properties can be referenced by a single element when necessary. Ply distortion of other defects can be modeled with a single element using this feature. The data hyperpatches for Euler angle data are specified by their identification number plus 1000 entered in the fields of the PPDE3 directive normally used for constant Euler angle data. Any entry less than 1000 is interpreted as angle in degrees constant over the element. It is important to check the arc angle data,  $\alpha$ , to make sure they are consistent with an axisymmetric involute. The PPDE3 directives for the Pagano example cone are shown in Table 6. Note that the tilt data are very nearly constant,  $\gamma \cong 12.55$ , Figure 12, and the associated Euler angle has been input on each PPDE3 directive as a constant,  $\theta = (90 - 12.55)$ . The connectivity data for each element are also shown in Table 6, and each element is constrained

TABLE 4. MATERIAL GEOMETRY DATAG DIRECT INPUT

DATAG, 1, , 1, -8.6, 2, -8.6, 3, -8.6	}	ARC ANGLE DATA $\psi = -(\alpha+\theta)$	
DATAG, 1, , 4, -7.6, 5, -6.7, 6, -6.1			
DATAG, 1, , 7, -5.5, 8, -5.1, 9, -4.7			
DATAG, 1, , 10, -4.3, 11, -4.1, 12, -3.8, 13, -3.5			
DATAG, 1, , 21, -7.2, 22, -7.2, 23, -7.2	}		
DATAG, 1, , 24, -6.2, 25, -5.5, 26, -4.9			
DATAG, 1, , 27, -4.5, 28, -4.1, 29, -3.9			
DATAG, 1, , 30, -3.7, 31, -3.6, 32, -3.4, 33, -3.3			
DATAG, 1, , 101, -23.6, 102, -23.6, 103, -23.6	}		
DATAG, 1, , 104, -22.6, 105, -21.7, 106, -21.1			
DATAG, 1, , 107, -20.5, 108, -20.1, 109, -19.7			
DATAG, 1, , 110, -19.3, 111, -19.1, 112, -18.8, 113, -18.5			
DATAG, 1, , 121, -22.2, 122, -22.2, 123, -22.2	}		
DATAG, 1, , 124, -21.2, 125, -20.5, 126, -19.9			
DATAG, 1, , 127, -19.5, 128, -19.1, 129, -18.9			
DATAG, 1, , 130, -18.7, 131, -18.6, 132, -18.4, 133, -18.3			
DATAG, 3, , 1, -5.4, 3, -23.7, 13, 0.0	}	HELIX ANGLE DATA	
DATAG, 3, , 21, 11.0, 23, -7.3, 28, 21.1, 33, 16.6			
DATAG, 3, , 101, -5.4, 103, -23.7, 113, 0.0			
DATAG, 3, , 121, 11.0, 123, -7.3, 128, 21.1, 133, 16.6			

TABLE 5. MATERIAL GEOMETRY DATA HYPERPATCH CONSTRUCTION

DLINPC, 1, 3, 1, 2, 3	}	LINEAR INTERPOLATION OF HELIX ANGLE DATA (SEE FIGURE 11)	
DLINPC, 2, 3, 3 THRU 13			
DLINPC, 3, 3,21,22,23			
DLINPC, 4, 3,23 THRU 28			
DLINPC, 5, 3,28 THRU 33			
DLINPC, 21, 3, 101 THRU 103	}		
DLINPC, 22, 3, 103 THRU 113			
DLINPC, 23, 3, 121 THRU 123			
DLINPC, 24, 3, 123 THRU 128			
DLINPC, 25, 3, 128 THRU 133			
DHPHEX,101,1, 1, 2,22,21,,,,,101,102,122,121	}	DATA HYPERPATCHES FOR ARC ANGLE DISTRIBUTION	
DHPHEX,102,1, 2, 3,23,22,,,,,102,103,123,122			
DHPHEX,103,1, 3, 4,24,23,,,,,103,104,124,123			
DHPHEX,104,1, 4, 5,25,24,,,,,104,105,125,124			
DHPHEX,105,1, 5, 6,26,25,,,,,105,106,126,125			
DHPHEX,106,1, 6, 7,27,26,,,,,106,107,127,126			
DHPHEX,107,1, 7, 8,28,27,,,,,107,108,128,127			
DHPHEX,108,1, 8, 9,29,28,,,,,108,109,129,128			
DHPHEX,109,1, 9,10,30,29,,,,,109,110,130,129			
DHPHEX,110,1,10,11,31,30,,,,,110,111,131,130			
DHPHEX,111,1,11,12,32,31,,,,,111,112,132,131			
DHPHEX,112,1,12,13,33,32,,,,,112,113,133,132			
DHPHEX,301,3, 1, 2,22,21,,,,,101,102,122,121	}	DATA HYPERPATCHES FOR HELIX ANGLE DISTRIBUTION	
DHPHEX,302,3, 2, 3,23,22,,,,,102,103,123,122			
DHPHEX,303,3, 3, 4,24,23,,,,,103,104,124,123			
DHPHEX,304,3, 4, 5,25,24,,,,,104,105,125,124			
DHPHEX,304,3, 5, 6,26,25,,,,,105,106,126,125			
DHPHEX,306,3, 6, 7,27,26,,,,,106,107,127,126			
DHPHEX,307,3, 7, 8,28,27,,,,,107,108,128,127			
DHPHEX,308,3, 8, 9,29,28,,,,,108,109,129,128			
DHPHEX,309,3, 9,10,30,29,,,,,109,110,130,129			
DHPHEX,310,3,10,11,31,30,,,,,110,111,131,130			
DHPHEX,311,3,11,12,32,31,,,,,111,112,132,131			
DHPHEX,312,3,12,13,33,32,,,,,112,113,133,132			

---

TABLE 6. FINITE ELEMENT PROPERTY AND CONNECTIVITY DEFINITION

---

PPDE3, 1,1, ,1101,77.45,1301  
 PPDE3, 2,1, ,1102,77.45,1302  
 PPDE3, 3,1, ,1103,77.45,1303  
 PPDE3, 4,1, ,1104,77.45,1304  
 PPDE3, 5,1, ,1105,77.45,1305  
 PPDE3, 6,1, ,1106,77.45,1306  
 PPDE3, 7,1, ,1107,77.45,1307  
 PPDE3, 8,1, ,1108,77.45,1308  
 PPDE3, 9,1, ,1109,77.45,1309  
 PPDE3,10,1, ,1110,77.45,1310  
 PPDE3,11,1, ,1111,77.45,1311  
 PPDE3,12,1, ,1112,77.45,1312

CPDE3, 1, 1, 2,22,21,,,CCX,101,102,122,121  
 CPDE3, 2, 2, 3,23,22,,,CCX,102,103,123,122  
 CPDE3, 3, 3, 4,24,23,,,CCX,103,104,124,123  
 CPDE3, 4, 4, 5,25,24,,,CCX,104,105,125,124  
 CPDE3, 5, 5, 6,26,25,,,CCX,105,106,126,125  
 CPDE3, 6, 6, 7,27,26,,,CCX,106,107,127,126  
 CPDE3, 7, 7, 8,28,27,,,CCX,107,108,128,127  
 CPDE3, 8, 8, 9,29,28,,,CCX,108,109,129,128  
 CPDE3, 9, 9,10,30,29,,,CCX,109,110,130,129  
 CPDE3,10,10,11,31,30,,,CCX,110,111,131,130  
 CPDE3,11,11,12,32,31,,,CCX,111,112,132,131  
 CPDE3,12,12,13,33,32,,,CCX,112,113,133,132

---

to be axisymmetric. The CCX mnemonic specified a 48 degree-of-freedom axisymmetric element bicubic in  $U_\theta$ ,  $U_r$ , and  $U_z$ . Additional constraints can be specified that in the case of LLX reduce the element to 12 degrees-of-freedom.

The modeling data for structural geometry, material geometry and finite element connectivity described in this section can be generated with the PDA/PATRAN-G program. Using an interactive graphics system for model generation and a preprocessor program for Euler angles, the bulk data for the Pagano example cone can be generated in less than 30 minutes elapsed time.

### 3.0 HOW TO ANALYZE YOUR INVOLUTE MODEL

The hard part is over. What remains are the boundary conditions, loads and case control directives necessary to analyze our model. The input data requirements are small in comparison to modeling the material geometry. An important point to remember is that all finite element geometry is three-dimensional (3-D) even though the displacement response is usually constrained axisymmetric. This primarily affects how surface and body forces are input to CCX elements in an exit cone analysis. However, the 3-D features remain to analyze specimens cut from involute rings or to model asymmetric cones.

#### 3.1 Modeling the Boundary Conditions

The torsional response or twisting of an involute introduces one more rigid body mode that must be constrained to avoid a singular stiffness matrix. Rigid body constraints,  $U_z = 0$  and  $U_\theta = 0$ , are the only constraints for free-standing billets and illustrate the use of single point constraint (SPC) directives. Any displacement component at a point may be specified zero or a prescribed value using the SPC1 or the SPC2 directive. To constrain the rigid body modes in the example cone, we could restrain  $U_\theta$  and  $U_z$  at grid point one,

SPC1,10,1,0.0, ,0.0

where

SPC1,SID,GID,U1,U2,U3

The set identification number is necessary to allow multiple boundary conditions in our bulk data deck. A case control directive is used to select which set of boundary conditions are active for each subcase. This is exactly the same as in NASTRAN. In our example case the coordinate directions are such that  $U_\theta = U1$  and  $U_z = U3$  at grid point one as a result of the geometry construction in Table 1. Note the blank field for U2 indicates the radial displacement component is unconstrained. If the direction of the constraint did not align with a coordinate axis, Euler angles would be input on fields following the displacements. Suppose we wanted to simulate a mold die surface by reacting the normal displacement at grid points on the outside of the billet. At a typical grid point, say 25, we would have

SPC1,10,25, ,0.0, ,1, , , -19.8

where a -19.8 degree rotation about the  $e_1$  axis aligns  $e_2'$  with the surface

normal at grid point 25. A detailed definition of all the fields is provided in the User's Manual.

Recall that in PATCHES most of the analysis points are not grid points. We must constrain mesh points as well as grid points on most models using the SPC2 directive. The next boundary point aft of grid point 28, for example, is mesh point 421 of element 8. The 421 is the IJK mnemonic for a mesh point in parametric coordinates which in this case is ( $\xi_1 = 1$ ,  $\xi_2 = 1/3$ ,  $\xi_3 = 0$ ). Each analysis point lies at a one-third point of the parametric coordinates and there are  $4 \times 4 \times 4 = 64$  of these mesh points. To constrain the normal at this point, we would have

SPC2,10,8,421, ,0.0, ,1, , , , -19.8

where as before the -19.8 degree rotation aligns  $\hat{e}_2$  with the surface normal. There are directives in PATCHES that constrain all the mesh points and grid points on one face of an element with one directive. Unfortunately we can only use surface constraint (SDC) directives on face five of CCX elements, i.e., the  $\theta = 0$  face. This restriction is temporary and will be removed in a later version.

In addition to single point boundary conditions, we need to be able to model sliding interfaces and periodic boundary conditions. Multipoint equality constraint (MPE) directives are used for this purpose in PATCHES. The joint between two extendible exit cones (EEC's), for example, has surfaces in contact that are not hard bonded. A linear model for sliding interfaces assumes frictionless contact such that the normal displacement components between surfaces are equal while the tangent plane displacement components are independent. To illustrate how the MPE directive is used to model this condition, consider the Pagano cone again but this time with a graphite insert in the forward cylindrical portion of the billet. Two additional elements model the insert, Figure 13, and we want to constrain  $U_r$  but not  $U_\theta$  and  $U_z$  to be equal on the cylindrical surface between grid point 1 and grid point 3. Note that since all elements in PATCHES are conforming elements we can insure this condition with mesh point equality constraints. In this case, 7 mesh points are constrained by the directives in Table 7. The format of the directive

MPE1,SID,UIJK,EIDP,IJKP,EIDS,IJKS

places the primary "P" points first followed by the secondary "S" points. The sliding interface modeled in Table 7 use MTRX directives to constrain all the

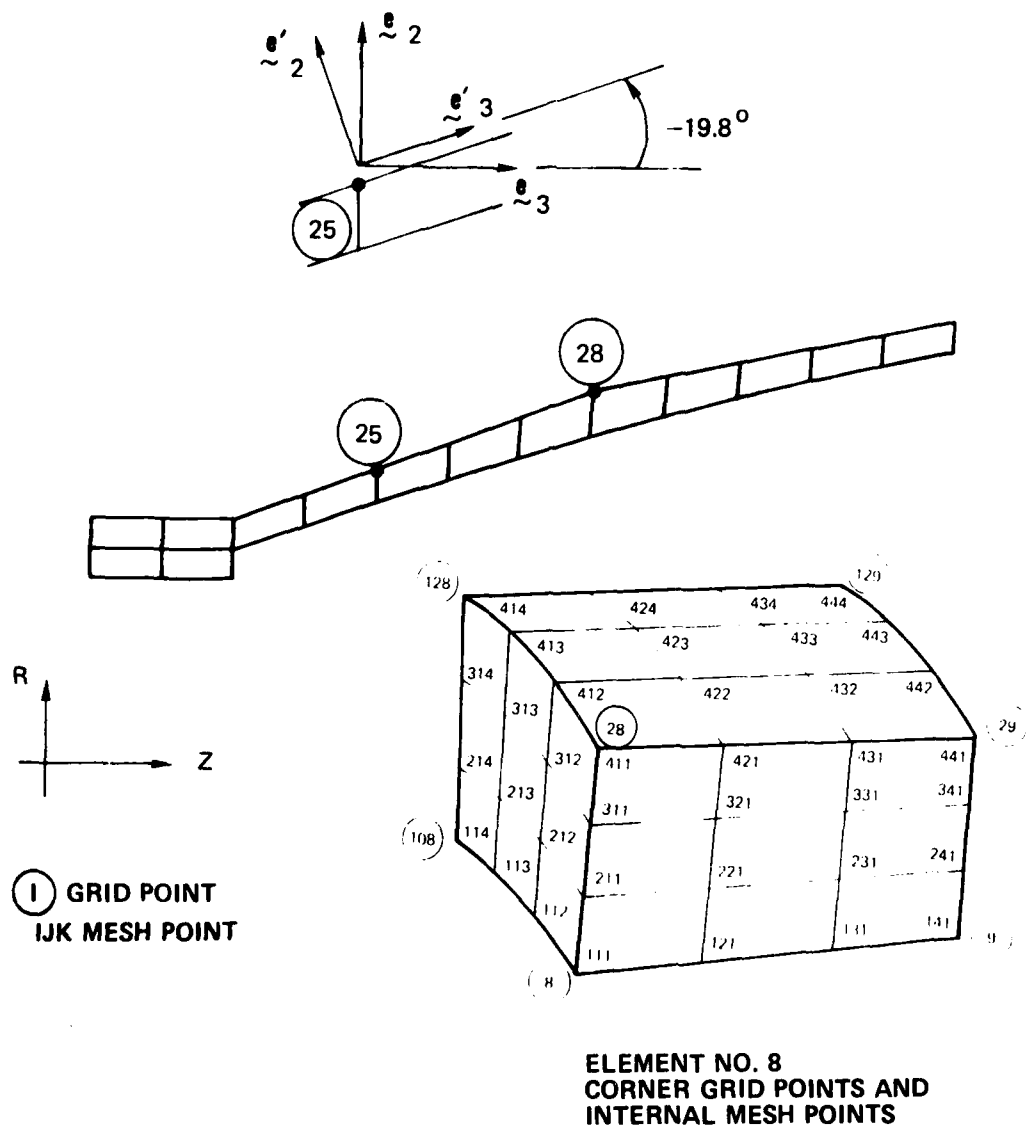


Figure 13. Model Cone with Cylindrical Insert

---

TABLE 7. SLIDING INTERFACE CONSTRAINT MODELING

---

MPE1\*,10,2,1,1051,13,1052  
MPE1 ,10,2,2,1053,14,1054  
MTRX-51,111,211,311,411  
MTRX-52,141,241,341,441  
MTRX-53,211,311,411  
MTRX-54,241,341,441

---

\*Note  $U_2 = U_r$  in the Pagano Example Cone

---



---

TABLE 8. ELEMENT TEMPERATURE MODELING

---

TEMP,5, 1,50	}	CONE
TEMP,5, 2,50		
TEMP,5, 3,50		
TEMP,5, 4,50		
TEMP,5, 5,50		
TEMP,5, 6,50		
TEMP,5, 7,50		
TEMP,5, 8,50		
TEMP,5, 9,50		
TEMP,5,10,50		
TEMP,5,11,50	}	CYLINDRICAL INSERT
TEMP,5,12,50		
TEMP,5,13,50,1.1		
TEMP,5,14,50,1.1		
DHPAT,50,P,40		
MTRX40,64(1000.0)		

---

boundary mesh points on a primary and secondary element at the same time. This is accomplished using an entry in the IJKP or IJKS fields greater than 1000 which indicates a list of IJK mesh points is to be used. These mesh points are input on a MTRX directive with identification number equal the entry less 1000. A detailed description of all the options for the MPE1 and MPE2 directives is provided in the User's Manual. When the constraint directions do not align with a coordinate axis, Euler angles can be input in a way similar to their input on SPC directives.

### 3.2 Modeling the Loads

Thermal loads are generated in PATCHES from data hyperpatches that define the temperature distribution within each element. Any distribution up to a tricubic can be input and a 3-D temperature hyperpatch is required even for CCX elements. If the temperature is constant, which is typical of a process stress analysis, the same data hyperpatch can be referenced by all elements. Table 8 shows a 1000°F pyrolysis temperature condition for all the elements in the example cone. Note the temperature in the sleeve elements are scaled to 1100 degrees to simulate a shrink fit.

The work equivalent thermal loads for an element in Cartesian coordinates are not distributed the way most people intuitively expect them to appear. Do not let this confuse you. A simple free thermal strain check in material coordinates can always be made if you want to confirm the accuracy of the thermal loads for an element. To do this, simply analyze a one element model with only rigid body constraints,  $U_\theta = U_z = 0$  at one mesh point, for a constant temperature rise over the element. The strain response in material coordinates should be  $\epsilon_i = \alpha_i \Delta T$ . Thermal loads are automatically generated for an element when a TEMP directive defines a temperature field for that element.

Mechanical loads can be input as grid point forces, distributed line loads, or distributed surface tractions and pressures. Each load directive has a set identification number for separating load conditions into individual subcases which may contain combinations of thermal and mechanical loads. Grid point loads are not normally used with CCX elements because of the axisymmetric assumption. They can be used with 3-D elements to analyze local stress concentrations at hardpoints or in point loaded test specimens. Keep in mind that a CCC element will respond to point loads with local deformations as well as structural. Unless you want to analyze a contact stress problem, a lower order

element should be used in the direction of a point load. This will result in a solution comparable to a thick shell analysis.

The most common mechanical loads are pressures. They are input using PLOAD3 directives which reference data patches for the distribution of pressure. These may be constructed from DATAG input just like the Euler angle data patches. These data can be constructed from data lines if the functional form of the pressure distribution is regular enough. Consider, for example, a pressure distribution in the Pagano case that decays from 10 psi to 2 psi at the exit plane. The distribution can be represented by a single parametric cubic,

$$p(\xi) = 8\xi^2 - 16\xi + 10$$

which we can input using a DLINE directive. All grid point values are computed from one data line as indicated in Table 9. These can then be referenced by DPATQ directives to form data patches and these in turn are referenced by PLOAD3 directives to generate work equivalent loads. Note the construction-in-context of ten data surface patches from one data line. Of course if the distribution were irregular, the values would be input at every mesh point. However, in many cases, like the above example, a considerable efficiency results from the construction features in PATCHES. In this case,  $p(Z)$  is represented by a single PC data line where  $Z = 1 + 5\xi$  relates axial station to the unit interval.

### 3.3 Case Control Input

The only input needed to analyze our model for the load conditions and boundary conditions just described are the case control directives. These directives define the conditions for analysis for each subcase and select the data for output. They also control the checkpoint-restart features of the program in multiple execution runs.

A very simple single run set of directives is shown in Table 10 for the Pagano example cone. The boundary conditions are specified by SDC, 10 which will activate all constraints in the bulk data with set identification number (SID) equal 10. The loads for this case are the collection of all bulk data for mechanical and thermal loads with SID equal 5. In our model, this would be a thermal load case. The DRY directive indicates literally a dry run in which the geometry, loads, properties, and connectivity directives are processed and can be output for checking. The ALL directive requests all this information in point format except for the material stiffness properties which were deleted

---

TABLE 9. ELEMENT PRESSURE LOAD MODELING

---

DLINE,51,5,A,0,8,-16,10, , 3 THRU 13  
DLINE,52,5,A,0,8,-16,10, ,123 THRU 133

DPATQ, 3,5, 3,123,124, 4  
DPATQ, 4,5, 4,124,125, 5  
DPATQ, 5,5, 5,125,126, 6  
DPATQ, 6,5, 6,126,127, 7  
DPATQ, 7,5, 7,127,128, 8  
DPATQ, 8,5, 8,128,129, 9  
DPATQ, 9,5, 9,129,130,10  
DPATQ,10,5,10,130,131,11  
DPATQ,11,5,11,131,132,12  
DPATQ,12,5,12,132,133,13

PLOAD3,5, 3, 3  
PLOAD3,5, 4, 4  
PLOAD3,5, 5, 5  
PLOAD3,5, 6, 6  
PLOAD3,5, 7, 7  
PLOAD3,5, 8, 8  
PLOAD3,5, 9, 9  
PLOAD3,5,10,10  
PLOAD3,5,11,11  
PLOAD3,5,12,12

---

---

TABLE 10. CASE CONTROL INPUT FOR A DRY RUN

---

TITLE, PAGANO EXACT INVOLUTE CONE  
SUBTITLE, USER'S GUIDE EXAMPLE  
TIME, 2  
SDC, 10  
LOAD, 5  
DRY  
OUTPUT  
ALL  
MATC,OFF  
BEGIN BULK

---

from the output by the MATC,OFF directive. If we did not want to see the material thermal expansion properties, we would add MATA,OFF to the case control input. Selective control of the output greatly reduces the number of pages of unnecessary printout. After a successful dry run, remove the DRY directive and change the TIME,2 to the number of minutes needed for the stress run. A good rule of thumb for involute models analyzed on a CDC 6600 is 0.70 minutes per element. This, of course, changes with element type and with restart runs.

Suppose we wanted to analyze two load conditions and then use superposition to combine the results in a third subcase. An example of this input is shown in Table 11. Note that the first subcase is the implied case always assumed to be input and does not require a SUBCASE directive. In this analysis, a unit axial load case and a unit pressure load case are solved and the results combined with appropriate scale factors to compare with test results. The element matrices are generated only once, two displacement solutions are generated and three stress cases are output. There are also features for combining cases from earlier runs that are described in the User's Manual.

There is a case control directive for axisymmetric models, AXY, that can be used to specify the angle subtended by the hyperpatch for all axisymmetric (CCX) finite elements. This angle is needed by the stiffness matrix generation module. The angle can also be input on a PARAM card in the bulk data deck. A typical input for the models described in the User's Guide is AXY,-15. Note that the angle must agree with the sense of the rotation from face 5 to face 6; i.e., from the  $\theta = 0$  face to the  $\theta \neq 0$  face.

---

TABLE 11. CASE CONTROL INPUT FOR MULTIPLE SUBCASES\*

---

TITLE, PAGANO/DAVIS INVOLUTE TEST CYLINDER  
SUBTITLE, SPECIMEN C UNIT AXIAL LOAD CASE  
TIME, 3  
SDC, 20  
LOAD, 30  
SUBCASE, 2  
SUBTITLE, SPECIMEN C UNIT PRESSURE CASE  
SDC, 20  
LOAD, 10  
SUBCASE, 3  
SUBTITLE, SPECIMEN C TEST C-3-103-1  
SUBCOM, -1.047, 0.163  
OUTPUT  
ALL  
BEGIN BULK

---

\*Note first subcase does not require SUBCASE card.

[This Page Intentionally Left Blank]

#### 4.0 APPLICATIONS AND ILLUSTRATIONS

Application of PATCHES-III to an involute test cylinder, a small exit cone billet and a beam test specimen cut from an involute ring are used to illustrate use of the program. These problems are small and focus on the fundamentals of involute analysis. Large production analyses, References 8 and 9, are described in contract reports. The User's Guide cases are small so that you can reanalyze the models for your own edification at modest computer cost.

##### 4.1 Involute Test Cylinder

One of the first applications of PATCHES-III to involutes also was used to verify the CCX finite elements. The structural assessment of involutes study, Reference 10, provided test data to validate the unusual strain response predicted analytically by Pagano. The gage section of the involute test cylinder was modeled with a single CCX element and subjected to three uniform load conditions: torsion, axial load, and internal pressure with excellent results, Reference 11. That same gage section is modeled in Figure 14 by two CCX elements. The extra element was needed for modeling an interleaf, not for accuracy, as described in Reference 8.

The input bulk data for the two element model are shown in Table 12 with four load conditions included in the model. Note the input of algebraic data hyperpatches to model the Euler angles rather than DHPHEX construction from input grid point values. Instead of 8 input DATAG values, we need only 3 nonzero entries to represent the same hyperpatch in algebraic format for a cylinder. The arc angle distribution

$$\alpha(\xi_1, \xi_2, \xi_3) = \Delta\alpha(\theta)\xi_3 + \Delta\alpha(r)\xi_2 + \alpha_0$$

is linear in radius,  $\xi_2$ , and rotational direction,  $\xi_3$ , and constant in the axial direction,  $\xi_1$ . The algebraic representation of the hyperpatch is simply

$$S_{443} = \Delta\alpha(\theta) \quad S_{344} = \Delta\alpha(r) \quad S_{444} = \alpha_0$$

with all other  $S_{ijk} = 0$ . The coefficients are sequenced as in a FORTRAN array. The other new feature illustrated by this case is the modeling of surface tractions with the FORCET directive. Surface tractions model the shear flow over a  $Z = \text{constant}$  surface for the torsion load case. Note the use of self equilibrating loads at opposite ends of the specimen. The warp-normal shear stress deformations and contours from the torsion case, Figures 15 and 16, illustrate the stress fields possible within a single element.

TABLE 12. INVOLUTE CYLINDER BULK DATA MODEL

CPDE3,1,1,4,3,2, , , ,CCX,13,16,15,14  
 CPDE3,2,2,3,6,5, , , ,CCX,14,15,18,17  
 GRID,1, ,0,2.1065 ,0  
 GRID,2, ,0,2.30736,0  
 GRID,3, ,0,2.30736,0.5  
 GRID,4, ,0,2.1065 ,0.5  
 GRID,5, ,0,2.4015 ,0  
 GRID,6, ,0,2.4015 ,0.5  
 PATCHQ,1,1,4,3,2  
 PATCHQ,2,2,3,6,5  
 HPR,1,1, , , ,0.0,15.0,-3  
 HPR,2,2, , , ,0.0,15.0,-3  
 DPATCH,10,A, 5,1,13,16, 4  
 DPATCH,31,A, 5,1, 2,14,13  
 DPATCH,32,A, 5,4, 3,15,16  
 DPATCH,33,A, 5,2, 5,17,14  
 DPATCH,34,A, 5,3, 6,18,15  
 DHPAT,10,A,10  
 DHPAT,20,A,20  
 MTRX 5,15(0.0),1000.0 } PRESSURE DATA  
 {MTRX10,47(0.0), -15.0,14(0.0),0.903565,-10.28222 }  $\Delta\alpha(\theta) = -15.0$   
 {MTRX20,47(0.0), -15.0,14(0.0), 0.37080, -9.37865 }  $\Delta\alpha(r) = 0.903565$   
 $\alpha_0 = -10.28222$   
 MATAL,2,1,1,8  
 MATOR,2,1,1,7  
 MTRX7, 2.8+6, 1.7+6, .625+6, .0395, .0413, .1066, } ELASTIC CONSTANTS  
 0.63+6,0.75+6,0.65+6  
 MTRX8, 0.8-6, 0.8-6, 2.4-6,3(0.0) } COEFFICIENTS OF THERMAL EXPANSION  
 PLOAD3,10,1,10 } PRESSURE LOAD  
 PLOAD3,30,1,31,-2.393558  
 PLOAD3,30,2,33,-2.393558  
 PLOAD3,30,1,32, 2.393558  
 PLOAD3,30,2,34, 2.393558  
 FORCET,40,1,31,-1.074144  
 FORCET,40,2,32,-1.074144  
 FORCET,40,1,33, 1.074144  
 FORCET,40,2,34, 1.074144  
 DHPAT,1,A,1  
 MTRX1,63(0.0),1000.0  
 TEMP,20,1,1  
 TEMP,20,2,1  
 PPDE3,1,2, ,1010,90.0,45.0  
 PPDE3,2,2, ,1020,90.0,45.0  
 SPC2,20,111,0, ,0  
 PARAM,ITER,350,AXY,-15.0  
 END DATA

THE COEFFICIENTS  
 ARE SEQUENCED AS  
 IN A FORTRAN  
 ARRAY; 111, 211,  
 ...,344,444.

SURFACE LOAD DATA PATCHES;  
 PRESSURE, AXIAL, TORSION

EULER ANGLE HYPERPATCHES

AXIAL LOAD

TORSION LOAD

THERMAL LOAD

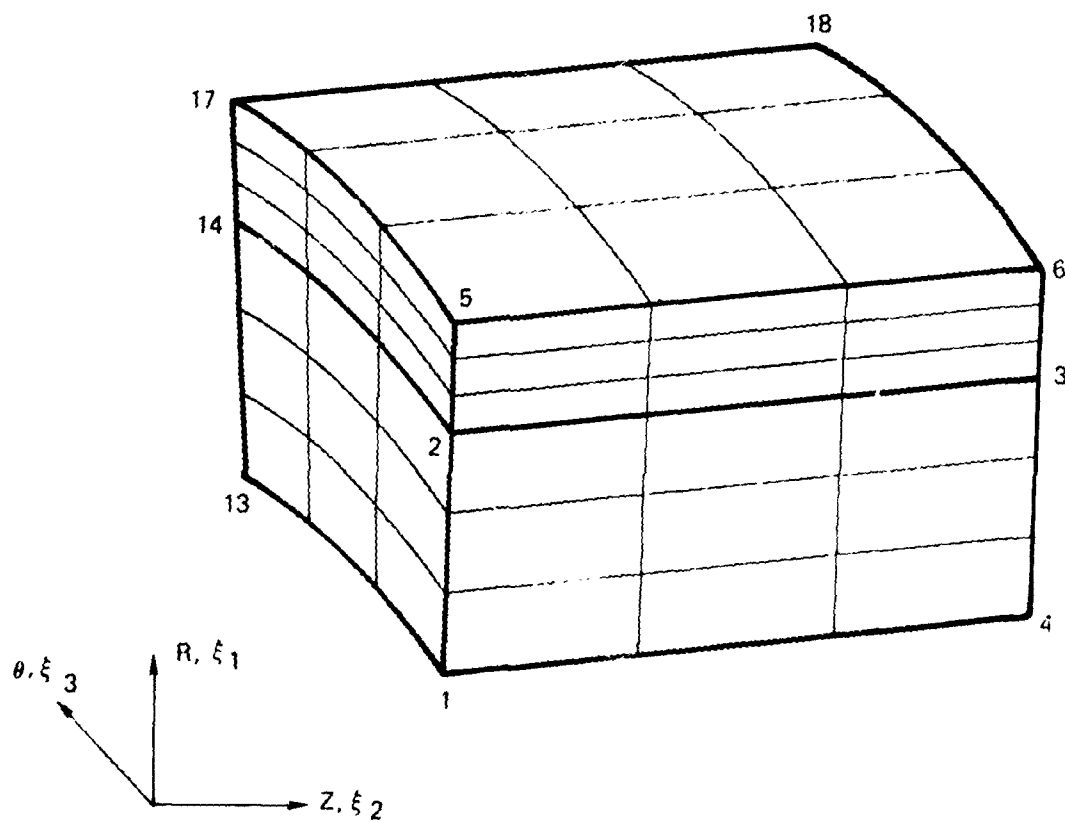


Figure 14. Involute Test Cylinder Gage Section Model

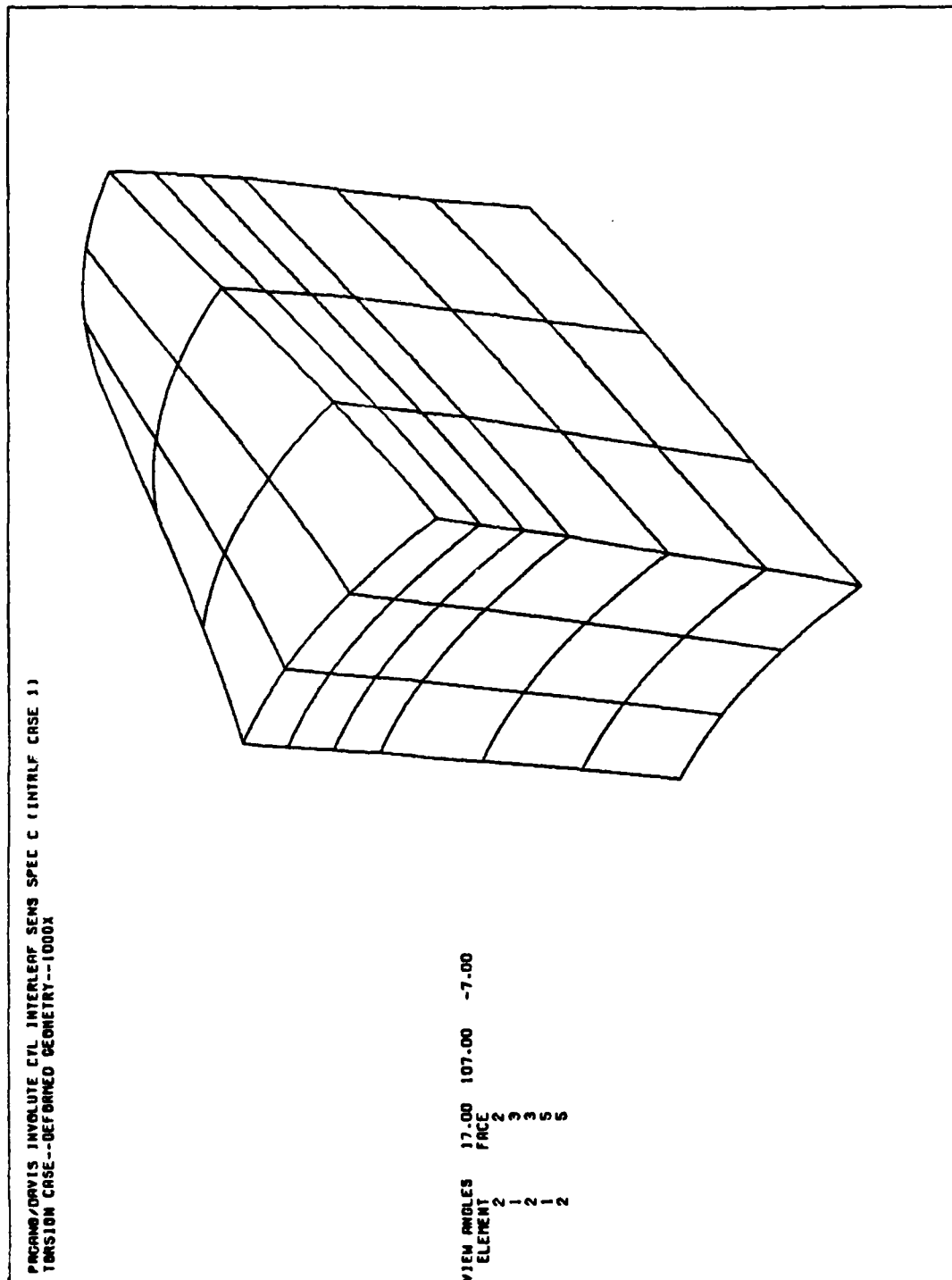
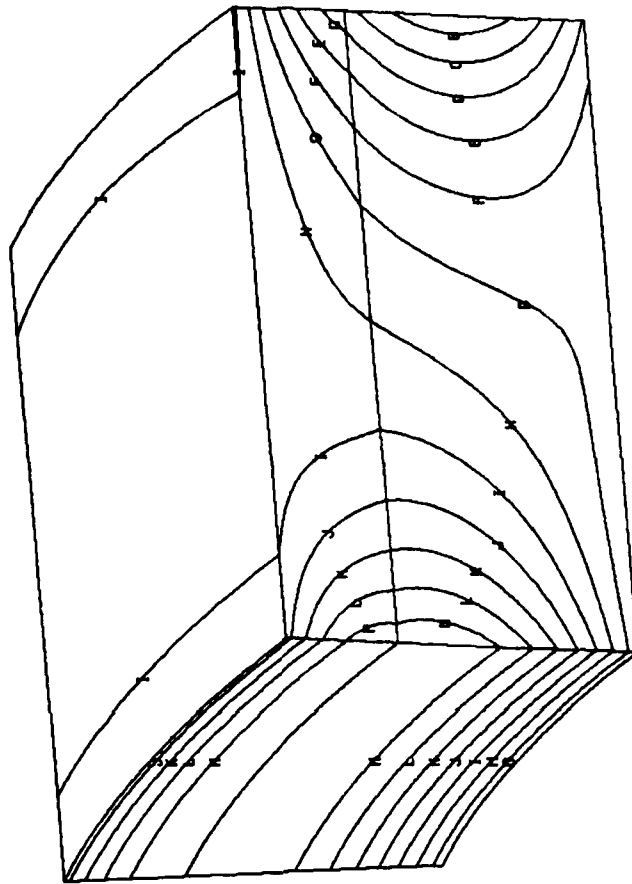


Figure 15. Involute Test Cylinder Deformations in Torsion

PAGRAM/DAVIS INVOLUTE CYL INTERLEAF SENS SPEC C (CONTROL CASE 1)  
TENSION CASE--FILL/NORMAL SHEAR STRESS



MATERIAL FRAME STRESS	623
VIEW ANGLE	17.00 107.00 -7.00
ELEMENT	FACE
2	1
1	2
2	3
1	5
2	6

15 CONTOUR INTERVALS

-0.160000E+03(A)	-0.165000E+03(B)
-0.150000E+03(C)	-0.145000E+03(D)
-0.140000E+03(E)	-0.135000E+03(F)
-0.130000E+03(G)	-0.125000E+03(H)
-0.120000E+03(I)	-0.115000E+03(J)
-0.110000E+03(K)	-0.105000E+03(L)
-0.100000E+03(M)	-0.950000E+02(N)
-0.900000E+02(O)	

Figure 16. Involute Test Cylinder Shear Stress Contours

The case control input for analysis of all four subcases on the same run are shown in Table 13. There is really nothing new in this analysis except the unusual number of subcases. It would save paper if MATC,OFF and MATA,OFF were used in the output control section since the properties are temperature independent in these analyses.

#### 4.2 Involute Billet Analysis

A CCAN size fixed cone billet of exact involute construction was designed by Pagano and processed into a carbon-carbon part. One of the early billet designs is described here that was later modified based on this PATCHES-III analysis of shrinkage stress during carbonization. The Euler angles for an exact involute or convolute can be computed directly for any radius and axial station based on the number of plies and involute constant. These data are omitted to save space, but the ply pattern for the 149 ply billet and  $C = 0.3$  involute constant is shown in Figure 17 with warp and fill directions marked. The finite element model is shown in Figure 18 in the meridional plane. There are nine CCX elements in the model.

The billet geometry is defined by the directives in Table 14. The construction is rather primitive and with a little effort the number of direct input grid points can be reduced. The temperature dependent properties that are different from Table 3 are shown in Table 15. Note the use of free thermal strain data for modeling the thermal expansion properties. The MATTAT directive is used for this option in place of the MATTA directive. The remaining finite element data are in Table 16. Interlaminar stress results for fill-normal shear and cross ply normal stress are shown in Figures 19 and 20. Although good strength data are not available for material in this condition, failures have occurred in billets at much lower stress levels. One of the design changes made to reduce these levels was to lower the arc angle by reducing the number of plies. The maximum arc angle in the design analyzed here is  $13^\circ$ , which is very high. The reason for the high arc angles is the large central angle required for lower arc angle designs. A large central angle caused layup and debulking problems.

These stress results are typical of the insight provided by analysis into the response of a particular billet design to processing. A simple model of the billet can often be constructed in a day or two if the material properties are available and the analyses are linear, which keeps computer costs reasonable without much accuracy loss.

---

TABLE 13. INVOLUTE TEST CYLINDER CASE CONTROL

---

TITLE, INVOLUTE TEST CYLINDER GAGE SECTION

SUBTITLE, TORSION LOAD CASE

TIME, 5

SDC, 20

LOAD, 40

SUBCASE, 2

SUBTITLE, PRESSURE LOAD CASE

LOAD, 10

SDC, 20

SUBCASE, 3

SUBTITLE, AXIAL LOAD CASE

LOAD, 30

SDC, 20

SUBCASE, 4

SUBTITLE, THERMAL LOAD CASE

LOAD, 20

SDC, 20

OUTPUT

ALL

BEGIN BULK

---

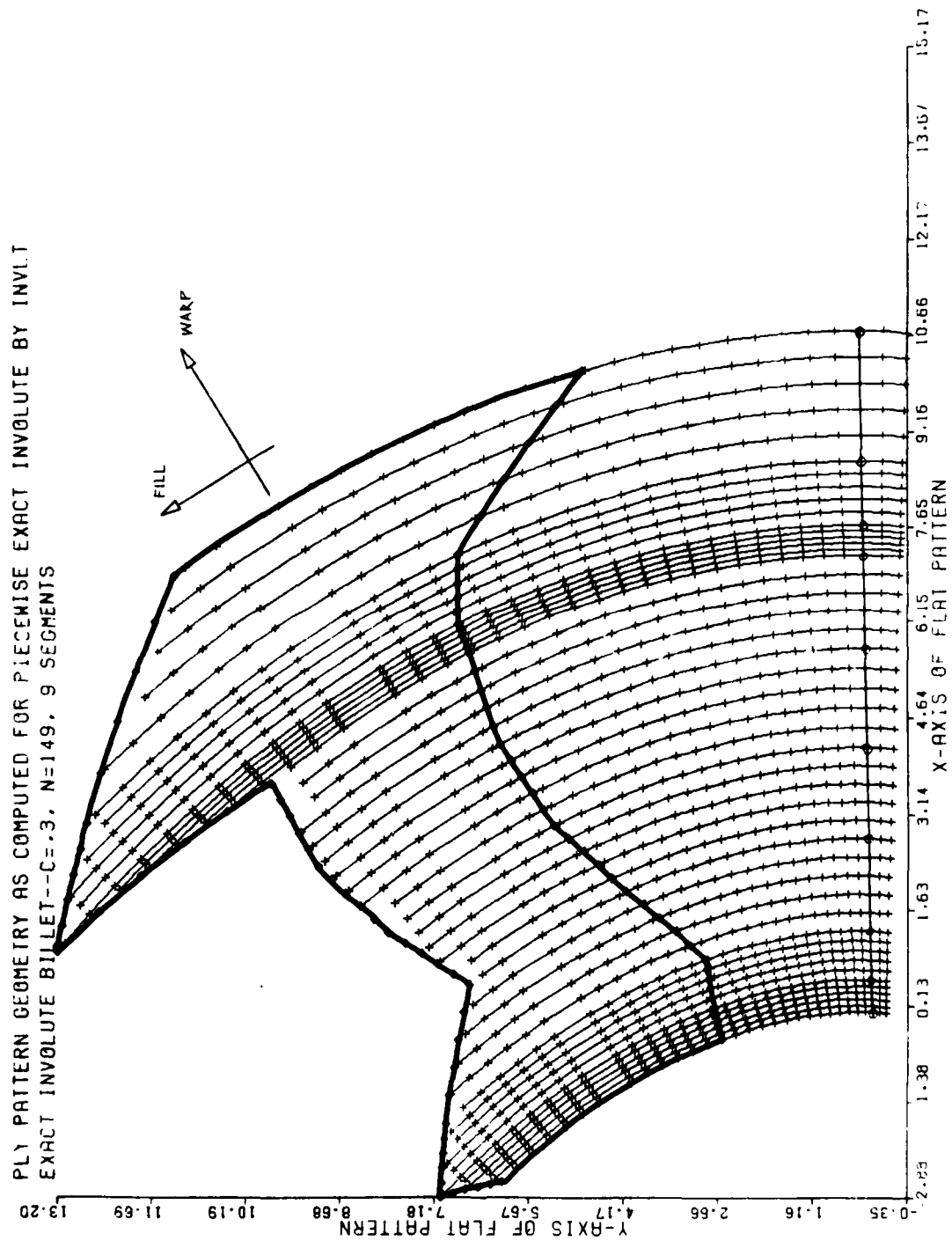


Figure 17. Exact involute Billet Ply Pattern

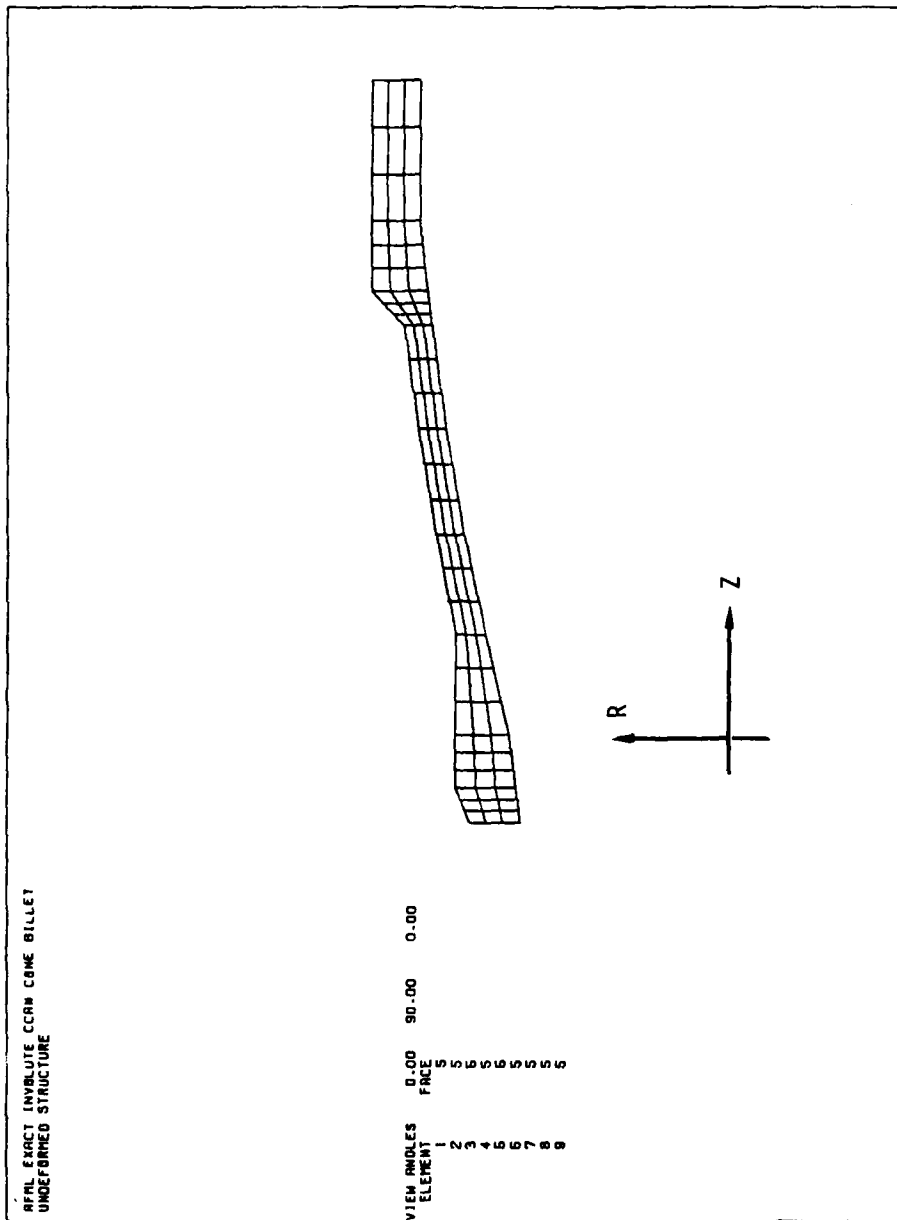


Figure 18. Exact Involute Billet Model

---

TABLE 14. INVOLUTE BILLET GEOMETRY MODEL

---

GRID, 1, , , 1.325, 0.0  
 GRID, 2, , , 1.387, 0.5  
 GRID, 3, , , 1.480, 1.25  
 GRID, 4, , , 1.839, 2.69  
 GRID, 5, , , 2.148, 4.10  
 GRID, 6, , , 2.406, 5.61  
 GRID, 7, , , 2.612, 7.08  
 GRID, 8, , , 2.680, 7.56  
 GRID, 9, , , 2.782, 8.56  
 GRID, 10, , , 2.782, 10.56  
 GRID, 11, , , 2.063, 0.0  
 GRID, 12, , , 2.063, 0.5  
 GRID, 13, , , 2.063, 1.25  
 GRID, 14, , , 2.063, 2.69  
 GRID, 15, , , 2.548, 4.10  
 GRID, 16, , , 2.806, 5.61  
 GRID, 17, , , 3.012, 7.08  
 GRID, 18, , , 3.482, 7.56  
 GRID, 19, , , 3.482, 8.56  
 GRID, 20, , , 3.482, 10.56

PATCHQ, 1, 1, 2, 12, 11  
 PATCHQ, 2, 2, 3, 13, 12  
 PATCHQ, 3, 3, 4, 14, 13  
 PATCHQ, 4, 4, 5, 15, 14  
 PATCHQ, 5, 5, 6, 16, 15  
 PATCHQ, 6, 6, 7, 17, 16  
 PATCHQ, 7, 7, 8, 18, 17  
 PATCHQ, 8, 8, 9, 19, 18  
 PATCHQ, 9, 9, 10, 20, 19

HPR, 1, 1, , , , 15.0, -3

....

....

HPR, 9, 9, , , , 15.0, -3

---

---

TABLE 15. INVOLUTE BILLET TEMPERATURE DEPENDENT PROPERTIES INPUT\*

---

DTPC, 9,70, 70,0.45+6,200,0.38+6,300,0.32+6, 400,0.26+6,500,0.21+6	} T,GIJ(T)
DTPC,10,70, 70,0.0 , 200,0.75-3, 300,0.90-3, 400,1.0-3, 500,1.1-3 , 750,1.2-3 , 1000,0.9-3,1250,0.0-3 ,1500,0.9-3	
DTPC,11,70, 70,0.00 , 200,1.2-3, 300,1.4-3, 400,1.5-3, 500,1.6-3, 750,1.8-3, 1000,1.703,1250,1.6-3,1500,1.6-3	} FREE THERMAL STRAIN; T,αIJΔT
DTPC,12,70, 70, 0.00 , 200, 3.0-3, 300, 4.8-3, 400, 3.6-3, 500, 0.0 , 750, -9.003, 1000,-10.5-3,1250,-11.0-3,1500,-11.0-3	

MATTO,1, ,1,2,3,4,5,6,7,8,9

MATTAT,1, ,10,11,12

---

\*Data Table Functions 1-8 are in Table 3.

---



---

TABLE 16. BILLET ELEMENT DATA

---

DATAG,1, ,1,-13.086,2,-12.492, .....

DATAG,3, ,1, 101.3,2, 101.7, .....

DHPHEX,101,1,1, 2,12,11, , , , ,101,102,112,111

DHPHEX,102,1,2, 3,13,12, , , , ,102,103,113,112

.....

.....

DHPHEX,109,1,9,10,20,19, , , , ,109,110,120,119

DHPHEX,301,3,1, 2,12,11, , , , ,101,102,112,111

.....

.....

DHPHEX,309,3,9,10,20,19, , , , ,109,110,120,119

PPDE3,1,1, ,1101,81.1,1301

.....

PPDE3,9,1, ,1109,81.1,1309

CPDE3,1,1, 2,12,11, , , , ,CCX,101,102,112,111

.....

CPDE3,9,9,10,20,19, , , , ,CCX,109,110,120,119

SPC2,10,1,111,0, ,0

---

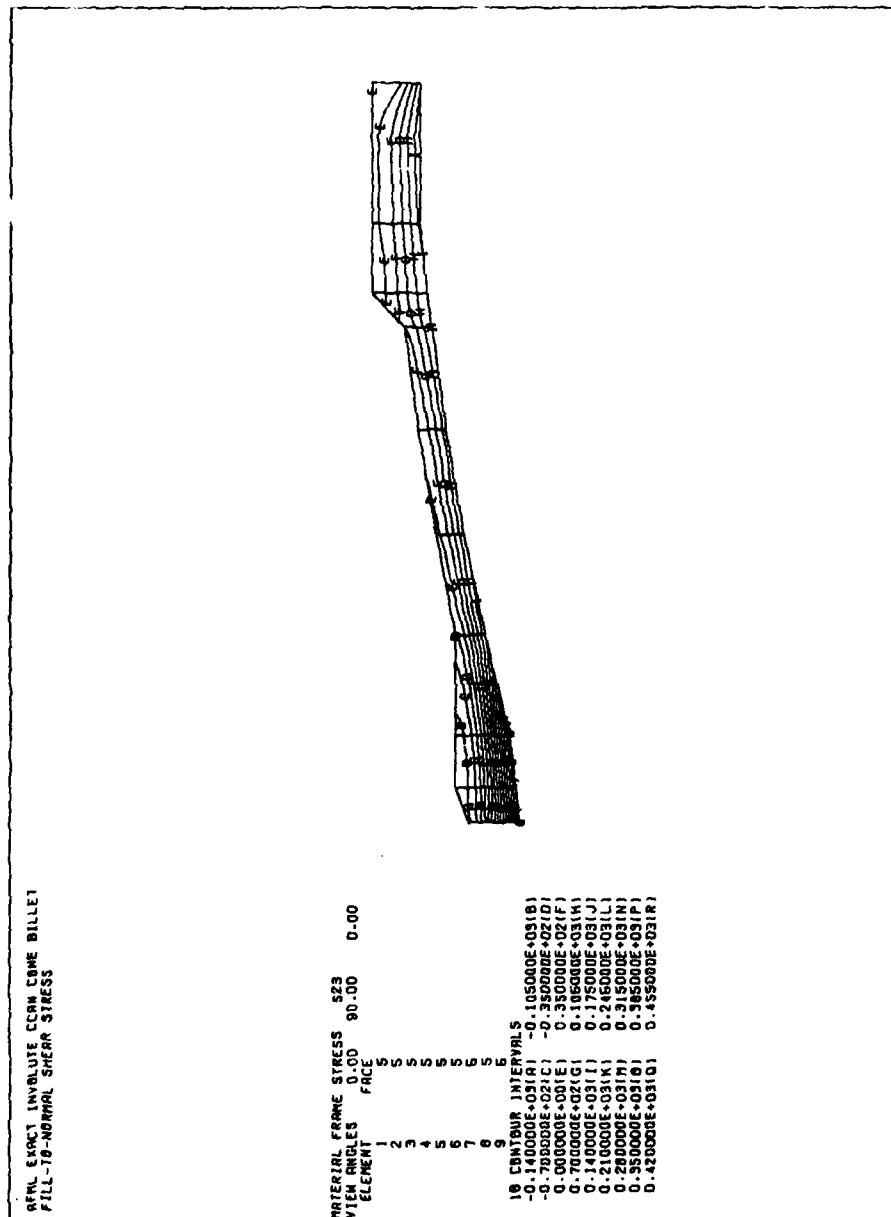


Figure 19. Involute Billet Shear Stress Contours

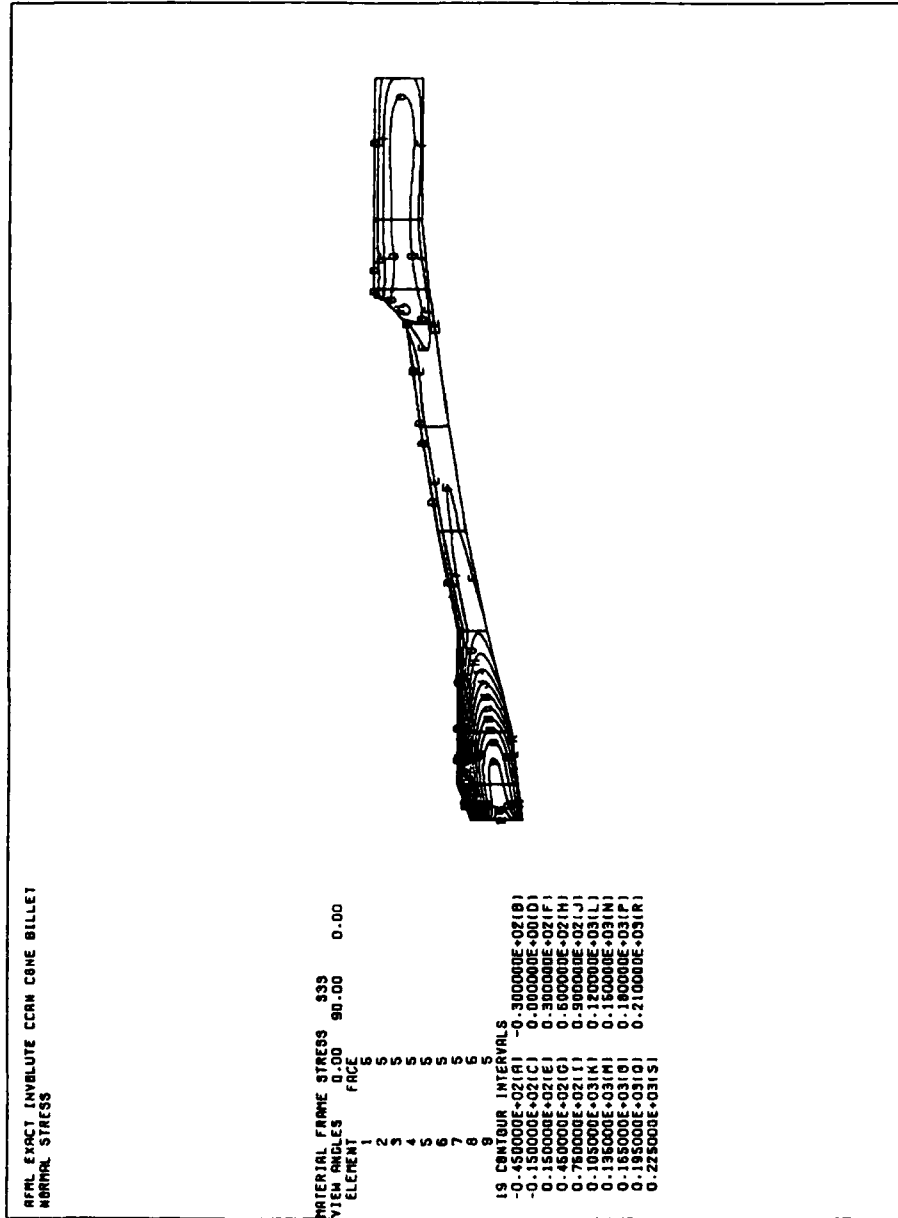


Figure 20. Involute Billet Normal Stress Contours

#### 4.3 Involute Beam Specimen

One of the nonaxisymmetric involute components that require analysis are specimens cut from involute billets and cones. A simple two element model of a curved beam specimen cut from an involute ring is shown in Figure 21. The specimen is a 30° sector cut from an extendable exit cone billet loaded by a concentrated force at its center. The LCC finite elements used to model the beam response impose a linear constraint in the radial direction. This removes the local contact stress response from the model. Physically it approximates using a pad to distribute the "point" load into the specimen without a stress singularity.

The input modeling directives are listed in Table 17 for the entire model. The helix angle and tilt angle are zero everywhere, and the arc angle varies from 2.2 degrees at the inside diameter to 2.8 degrees at the outside diameter. The boundary conditions are pinned on one end and rollers on the other end. The fill stress and the fill-normal shear stress contours are shown in Figures 22 and 23. These photoelastic like figures are used to help design specimen geometry and support fixtures to give a desired stress state. Once a specimen design has been found, a more detailed model can be constructed, if necessary, for data reduction.

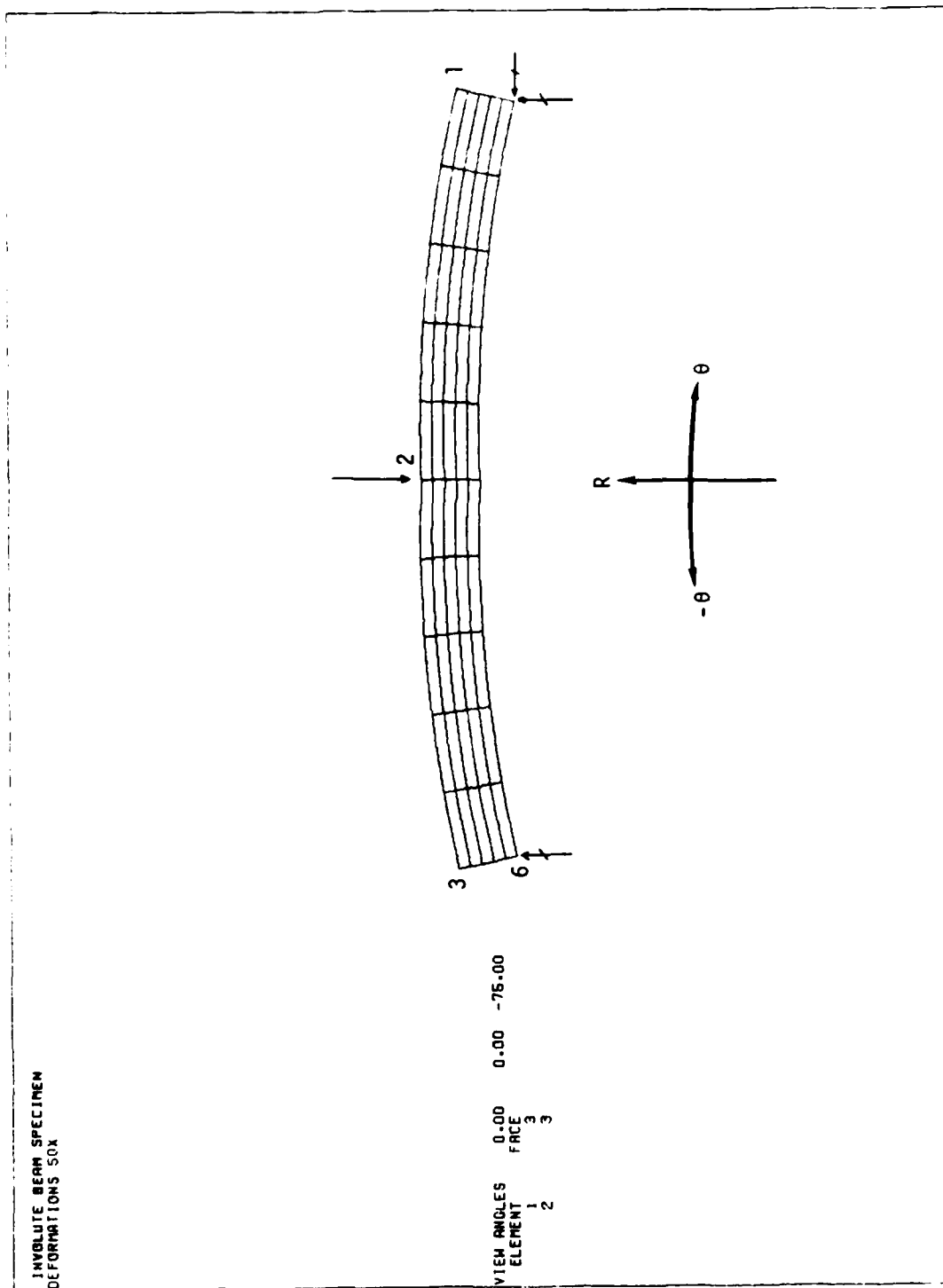


Figure 21. Involute Beam Specimen Model

---

TABLE 17. INVOLUTE BEAM MODELING DIRECTIVES

---

```

GRID, 1, , ,20.994,0.0
GRID, 4, , ,20.158,0.0
GRID, 7, , ,20.994,1.0
GRID,10, , ,20.158,1.0
PATCHQ,1,4,10,7,1
HPR,1,1, , , ,0.0,15.0,-3
HPR,2,1, , , ,15.0,30.0,-3
DATAG,1, , 1, -2.2,4, -2.28,7, -2.2,10, -2.28,
        2,-17.2,5,-17.28,8,-17.2,11,-17.28,
        3,-32.2,6,-32.28,9,-32.2,12,-32.28
DHPHEX,1,1,4,10,7,1, , , ,5,11,8,2
DHPHEX,2,1,5,11,8,2, , , ,6,12,9,3
MATOR,1,1,1,1
MTRX1,2.8 +6,1.7 +6,0.7 +6,0.037,0.23,0.35,
        0.59+6,0.76+6,0.60+6
PPDE3,1,1, ,1001,90.0,90.0
PPDE3,2,1, ,1002,90.0,90.0
CPDE3,1,4,10,7,1, , , ,LCC,5,11,8,2
CPDE3,2,5,11,8,2, , , ,LCC,6,12,9,3
FORCE,5,2, , -100.0
FORCE,5,8, , -100.0
SPC1,10, 4,0,0,0
SPC1,10,10,0,0,0
SPC1,10,12, ,0
SPC1,10, 6, ,0
END DATA

```

DATA  
HYPERPATCHES  
FOR ARC ANGLE  
DISTRIBUTION

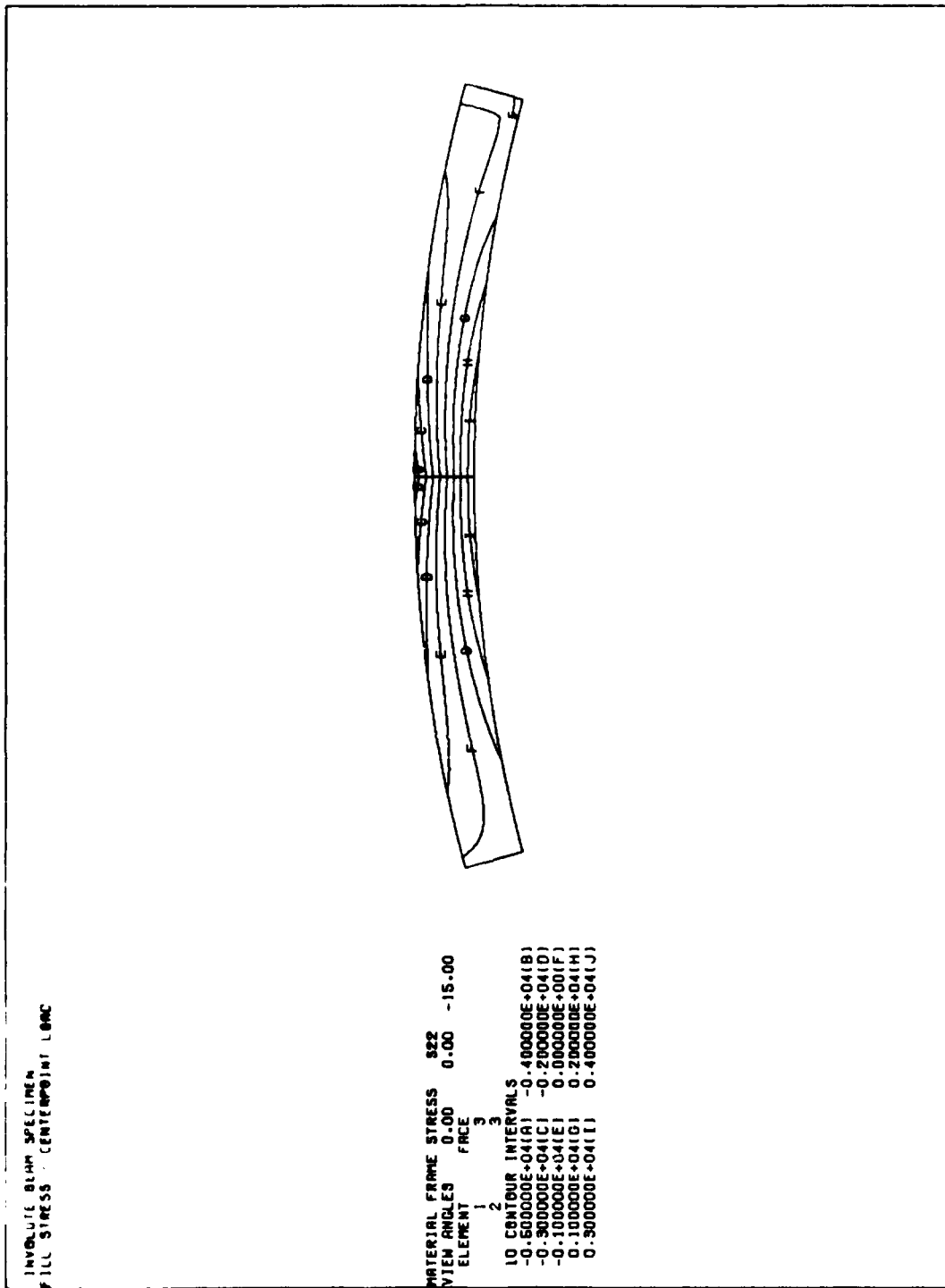


Figure 22. Involute Beam Fill Stress Contours

INVOLUTE BEAM SPECIMEN  
FILL-NORMAL SHEAR STRESS / CENTERPOINT LOAD

MATERIAL FRAME STRESS 323  
VIEW ANGLES 0.00 0.00 -15.00  
ELEMENT FACE

ELEMENT	FACE	STRESS
1	1	0.00000E+00
2	2	0.00000E+00
3	3	0.00000E+00
27 CONTOUR INTERVALS		
-0.275000E+03	(A)	-0.250000E+03
-0.225000E+03	(C)	-0.200000E+03
-0.175000E+03	(E)	-0.150000E+03
-0.125000E+03	(G)	-0.100000E+03
-0.075000E+03	(I)	-0.050000E+03
-0.025000E+03	(K)	0.000000E+00
0.025000E+03	(M)	0.050000E+03
0.075000E+03	(O)	0.100000E+03
0.125000E+03	(Q)	0.150000E+03
0.175000E+03	(S)	0.200000E+03
0.225000E+03	(U)	0.250000E+03
0.275000E+03	(W)	0.300000E+03
0.325000E+03	(Y)	0.350000E+03
0.375000E+03	(Z)	0.400000E+03



Figure 23. Involute Beam Shear Stress Contours

## 5.0 UNDERSTANDING THE RESULTS

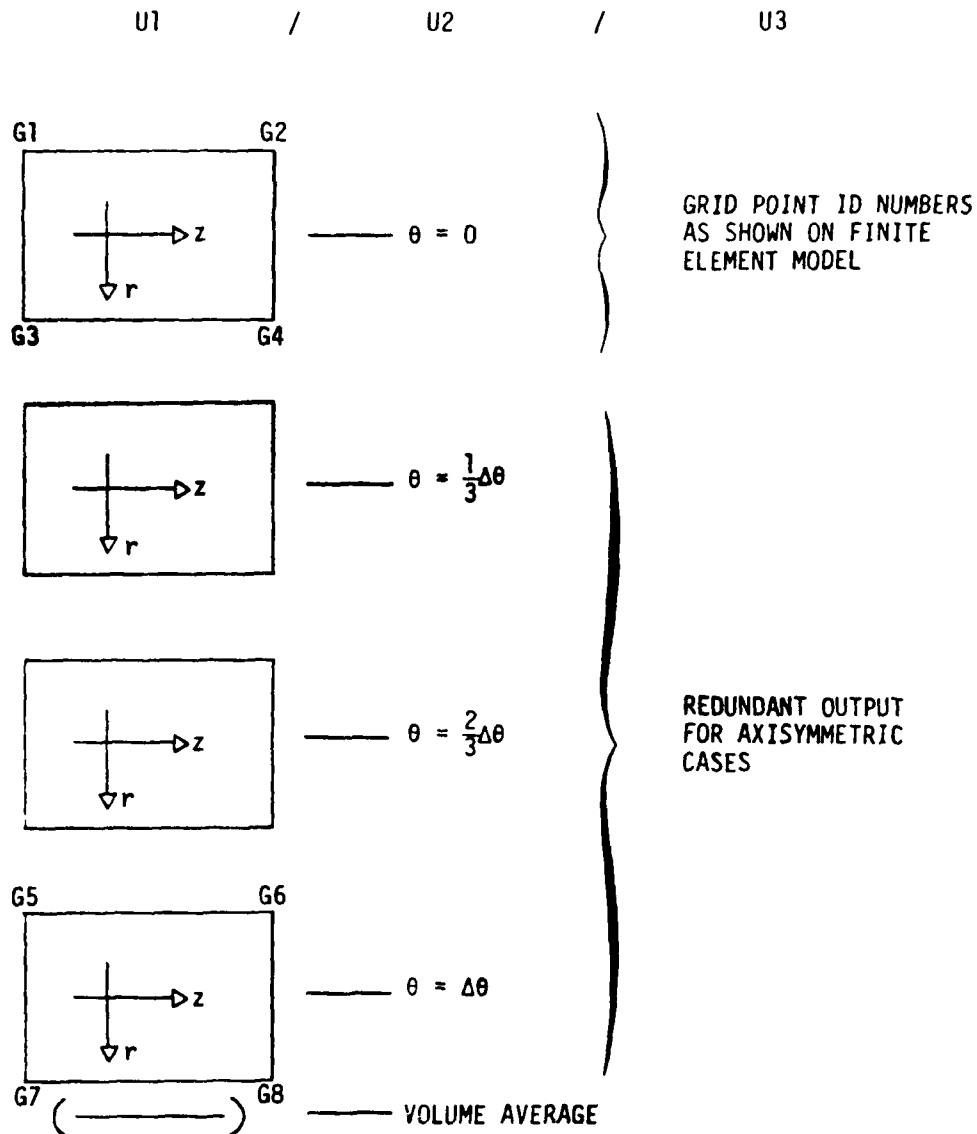
The analysis of involutes is obviously complicated by the torsional response mode and the unusual material distribution. Also the 3-D stress-strain response can be very difficult to evaluate; especially if only printed output is available. The most significant result is usually not the maximum stress because of the low interlaminar strength of carbon-carbon involutes. There is no easy solution to this problem. We can, however, suggest basic approaches to printing and plotting the output that will make the analyst's job less difficult.

### 5.1 Printed Output

Point format is used for all PATCHES solution data. This means 64 numbers for each element for each component function. Just the organization of the data on a page of printout can be confusing. The grid point identification numbers for the 8 corner nodes are output with the first component of every category of solution data printed. Table 18 shows the layout and indicates the directions of increasing radius and axial station within the printout for CCX elements. Each block represents 16 of the 64 values, and they correspond to constant  $\theta$  planes. A simplified output for CCX elements to eliminate redundant output is obviously needed. The most important output are the material frame stresses and strains. They can be related directly to material strength data. The values are recovered at all 64 mesh points for plotting purposes. The stress accuracy of a displacement method element probably warrants stress recovery at only 27 mesh points, but in either case, variable, even singular, strain fields are modeled well by a single element. Unless otherwise noted, the total strains are output in thermal load cases. Also, keep in mind that the displacements are output in Cartesian, not cylindrical, coordinates.

The quality of a solution is reflected in the convergence characteristics of the solution. If it converges to the default precision, it is numerically an excellent result. If this takes more than N cycles, either the material or the model is highly anisotropic. This happens often with carbon-carbon materials. If the iteration is not fully converged, the results may still be useful. The form if not the exact magnitude of the response can usually be determined from such cases. When the iteration does not converge after 2N or more cycles, it usually means there is a near singularity in the model which should be found and eliminated.

TABLE 18. PATCHES-III OUTPUT FORMAT FOR CCX ELEMENTS



Remarks:

1. The stress-strain output is axisymmetric in the material coordinate frame, but not in the Cartesian coordinate frame.
2. The Cartesian coordinate frame output is equal to cylindrical coordinate frame output on the  $\theta = 0$  plane.

## 5.2 Plotted Output

PATCHES plotted output is produced by a postprocessor program, PATPLOT, from a data file created automatically during a run. Three kinds of plots are possible, deformed geometry, carpet, i.e., data surface plots and contour plots. Any combination of elements and element surfaces may be included in a plot. The system is designed for use from a CRT terminal where the user responds to prompts for plot definition information for each frame.

Even when using CCX elements the full 3-D display capability exists for every element. A deformed geometry plot, Figure 24, of an ENEC joint, Reference 8, indicates the detail that can be included in a single figure. Normally the RZ or profile view of face 5 is used for stress-strain contours for multiple element views. Often a single element will be displayed to show interelement contours in the nature of an excised photoelastic stress picture, Figure 25. These plots provide insight into the material response that cannot be obtained from printed output.

It is often helpful to have XY plots of a stress component through the thickness or as a function of station. These are not available from PATPLOT. Such plots are especially helpful when comparing results for similar but not identical cones or when evaluating stress sensitivity to material changes. An example of interlaminar stress sensitivity to prepreg shrinkage properties, Figure 26, shows the utility of such plots.

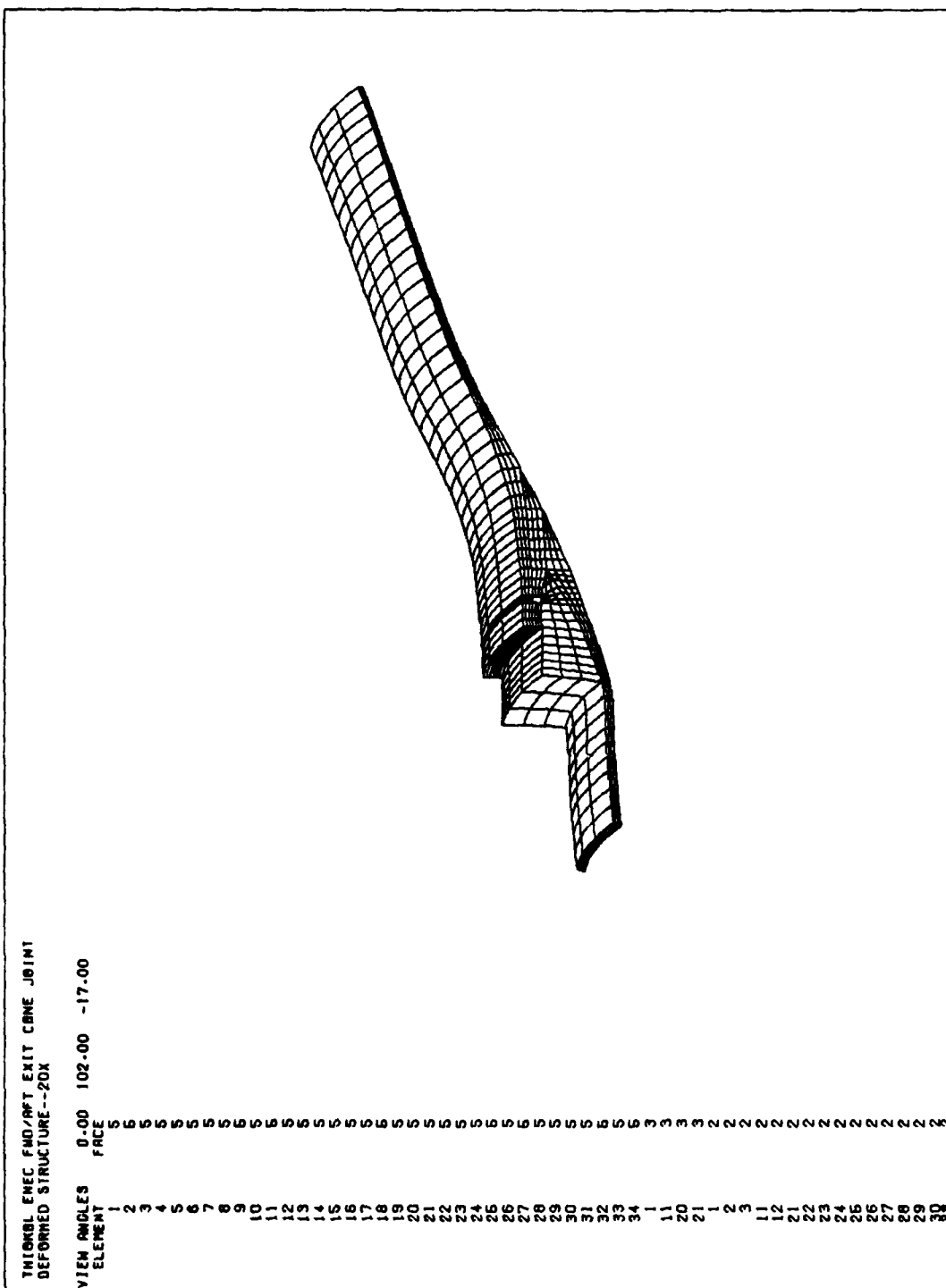


Figure 24. ENEC Joint Finite Element Model Deformations

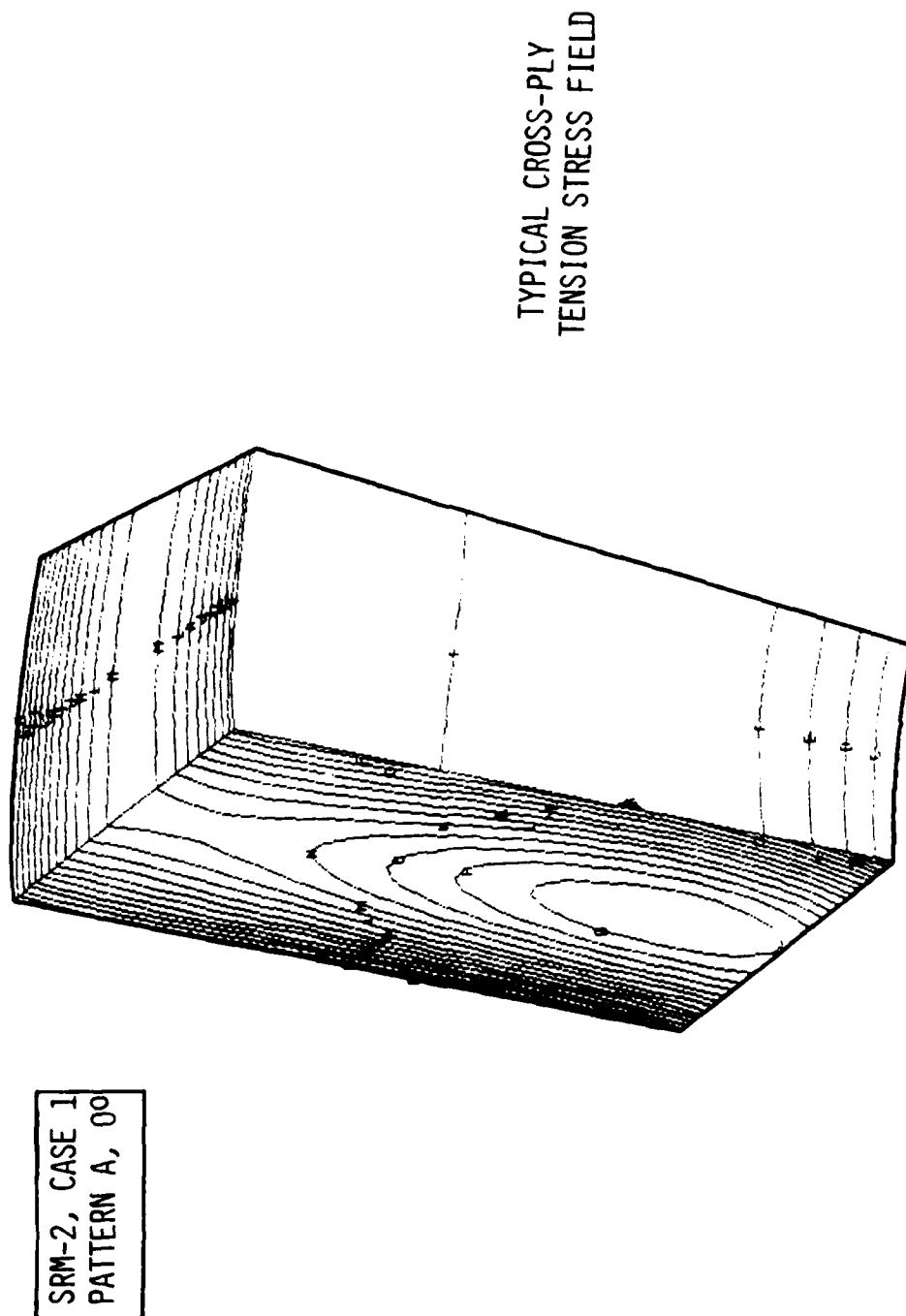


Figure 25. Contour Stress Results for a Single CCX Element

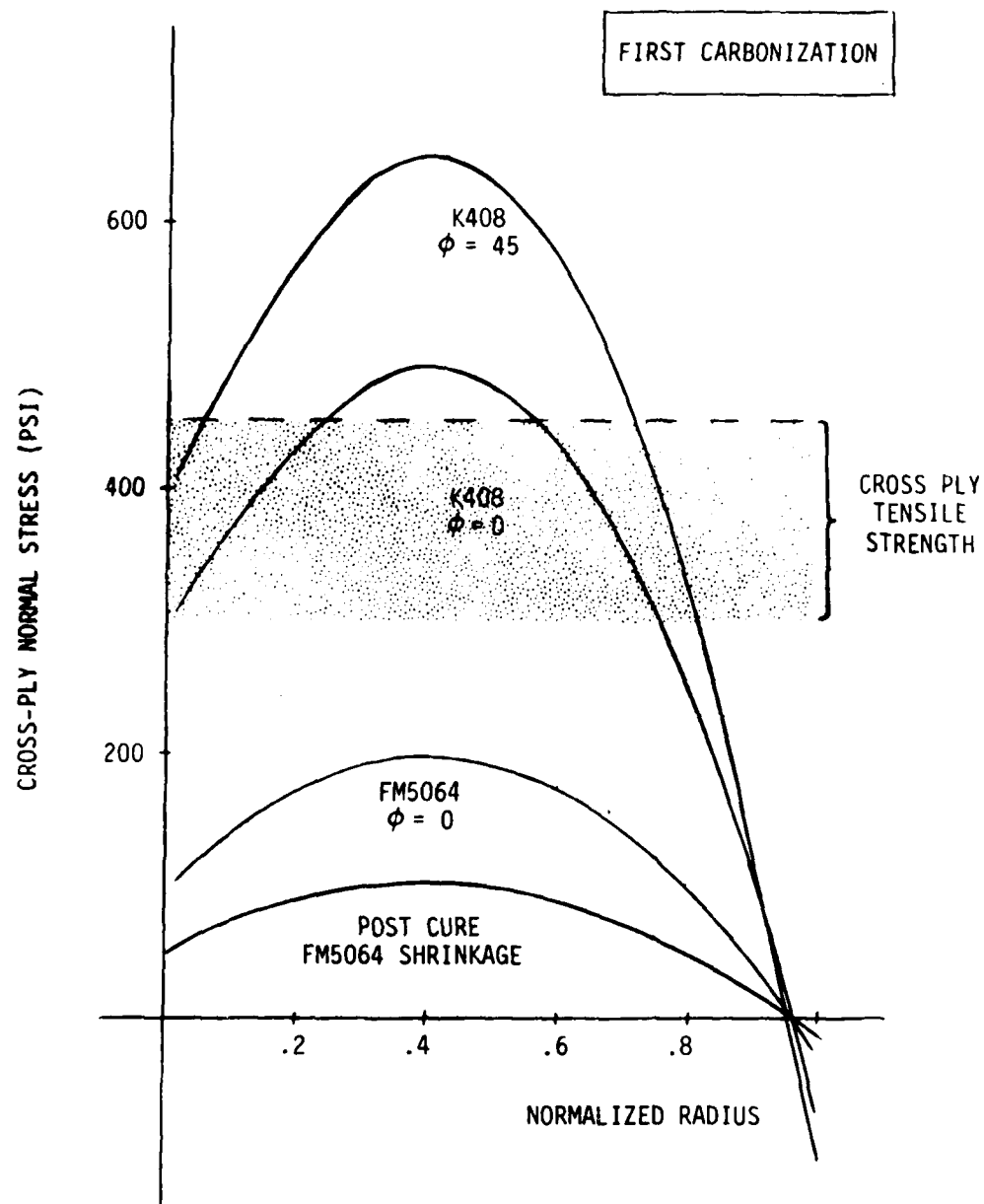


Figure 26. Involute Cylinder Shrinkage Study

1. Stanton, E. L. and N. J. Pagano, "Curing Stress Fields in Involute Exit Cones," Modern Developments in Composite Materials and Structures, J. R. Vinson, Ed., ASME Winter Annual Meeting, 1979.
2. Pagano, N. J., "Exact Involute Bodies of Revolution," to be published.
3. Savage, E. E., "The Geometry of Involute Construction," presented at the First JANNAF Carbon-Carbon Rocket Nozzle Technology Subcommittee Meeting, Monterey, CA, October 1979.
4. Buch, J. D. and W. H. Pfeifer, "Process Stresses as Revealed by Microstructure and Microcracking," AFML Conference on Analysis and Fabrication of Carbon-Carbon Involute Exit Cones, Dayton, Ohio, February 1979.
5. Stanton, E. L., L. M. Crain and T. F. Neu, "A Parametric Cubic Modelling System for General Solids of Composite Materials," Int. J. Num. Meth. Engng., Vol. 11, 1977, pp. 653-670.
6. Stanton, E. L. and L. M. Crain, "PATCHES-III User's Manual," PDA Engineering, AFRPL-TR-81-42, April 1981.
7. Shepler, R. E., M. K. Towne and D. K. Saylor, "Carbon-Fiber Composites," Machine Design, May 1979.
8. Kipp, T. E. and E. L. Stanton, "Finite Element Spiral Ply Composites," PDA Engineering, AFRPL-TR-81-38, April 1981.
9. Stanton, E. L. and T. E. Kipp, "Low-Risk Carbon-Carbon Exit Cone Construction Program," PDA Report TR-1484-00-01, January 1981.
10. Davis, H. O. and D. Vronay, "Structural Assessment of Involutes," AFML-TR-79-4068, June 1979.
11. Stanton, E. L. and R. L. Holman, "Involute Exit Cone Processing Stress and Deformation Studies," JANNAF 1st Carbon/Carbon Nozzle Technology Meeting, October 1979.

DATE  
FILMED  
8